

## Accepted Manuscript

CD36 palmitoylation disrupts free fatty acid metabolism and promotes tissue inflammation in non-alcoholic steatohepatitis

Lei Zhao, Chang Zhang, Xiaoxiao Luo, Pei Wang, Wei Zhou, Shan Zhong, Yunxia Xie, Yibo Jiang, Ping Yang, Renkuang Tang, Qin Pan, Andrew R. Hall, Tu Vinh Luong, Jiangaofan, Zac Varghese, John F. Moorhead, Massimo Pinzani, Yaxi Chen, Xiong Z. Ruan

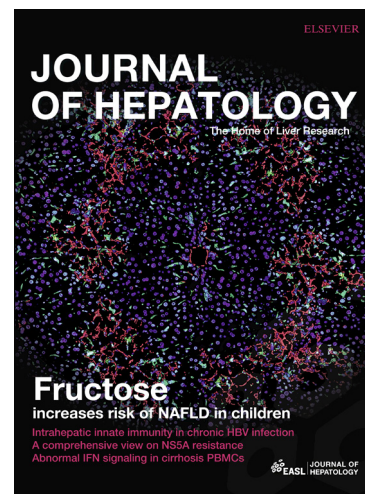
PII: S0168-8278(18)32014-2  
DOI: <https://doi.org/10.1016/j.jhep.2018.04.006>  
Reference: JHEPAT 6937

To appear in: *Journal of Hepatology*

Received Date: 12 September 2017  
Revised Date: 8 March 2018  
Accepted Date: 3 April 2018

Please cite this article as: Zhao, L., Zhang, C., Luo, X., Wang, P., Zhou, W., Zhong, S., Xie, Y., Jiang, Y., Yang, P., Tang, R., Pan, Q., Hall, A.R., Luong, T.V., Fan, J., Varghese, Z., Moorhead, J.F., Pinzani, M., Chen, Y., Ruan, X.Z., CD36 palmitoylation disrupts free fatty acid metabolism and promotes tissue inflammation in non-alcoholic steatohepatitis, *Journal of Hepatology* (2018), doi: <https://doi.org/10.1016/j.jhep.2018.04.006>

This is a PDF file of an unedited manuscript that has been accepted for publication. As a service to our customers we are providing this early version of the manuscript. The manuscript will undergo copyediting, typesetting, and review of the resulting proof before it is published in its final form. Please note that during the production process errors may be discovered which could affect the content, and all legal disclaimers that apply to the journal pertain.



## **CD36 palmitoylation disrupts free fatty acid metabolism and promotes tissue inflammation in non-alcoholic steatohepatitis**

Lei Zhao<sup>1</sup>, Chang Zhang<sup>1</sup>, Xiaoxiao Luo<sup>1</sup>, Pei Wang<sup>1</sup>, Wei Zhou<sup>1</sup>, Shan Zhong<sup>1</sup>, Yunxia Xie<sup>1</sup>, Yibo Jiang<sup>3</sup>, Ping Yang<sup>1</sup>, Renkuang Tang<sup>1</sup>, Qin Pan<sup>4</sup>, Andrew R Hall<sup>5</sup>, Tu Vinh Luong<sup>6</sup>, Jiangao Fan<sup>4</sup>, Zac Varghese<sup>7</sup>, John F. Moorhead<sup>7</sup>, Massimo Pinzani<sup>5</sup>, Yaxi Chen<sup>1,\*†</sup>, Xiong Z. Ruan<sup>1,2,7,\*†</sup>

<sup>1</sup>Centre for Lipid Research & Key Laboratory of Molecular Biology for Infectious Diseases (Ministry of Education), Institute for Viral Hepatitis, Department of Infectious Diseases, the Second Affiliated Hospital, Chongqing Medical University, 400016 Chongqing, China; <sup>2</sup>The Collaborative Innovation Center for Diagnosis and Treatment of Infectious Diseases (CCID), Zhejiang University, 310058 Hangzhou, China; <sup>3</sup>Astra Zeneca-Shenzhen University Joint Institute of Nephrology, Centre for Nephrology, Shenzhen University Medical School, Shenzhen University, Shenzhen, China; <sup>4</sup>Department of Gastroenterology, Xinhua Hospital, Shanghai Jiaotong University School of Medicine, 200092 Shanghai, China; <sup>5</sup>Sheila Sherlock Liver Centre, Royal Free London NHS Foundation Trust and UCL Institute for Liver and Digestive Health, University College London Medical School, Royal Free Campus, University College London, London NW3 2PF, United kingdom; <sup>6</sup>Department of Cellular Pathology, Royal Free London NHS Foundation Trust, London, UK; <sup>7</sup>John Moorhead Research Laboratory, Centre for Nephrology, University College London Medical School, Royal Free Campus, University College London, London NW3 2PF, United kingdom.

\* Corresponding authors. Addresses: Centre for Lipid Research & Key Laboratory of Molecular Biology for Infectious Diseases (Ministry of Education), Institute for Viral Hepatitis, Department of Infectious Diseases, the Second Affiliated Hospital, Chongqing Medical University, 400016 Chongqing, China. E-mail addresses: cheniyaxi@cqmu.edu.cn (Y.Chen), x.ruan@ucl.ac.uk (X.Z. Ruan)

† These authors share co-senior authorship.

**Keywords:** fatty acid translocase CD36; non-alcoholic steatohepatitis; palmitoylation.

Financial support

This work was supported by the National Natural Science Foundation of China (Key Program, No. 81390354, 81570517, 31640043 and 31540029), Kidney Research UK (RP46/2015) and Chongqing Research Program of Basic Research and Frontier Technology (No. cstc2016jcyjA0545 & cstc2015jcyjBX0044).

Conflict of interest

The authors who have taken part in this study declare that they do not have anything to disclose regarding funding or conflict of interest with respect to this manuscript.

Authors' contributions

LZ, CZ, XXL, PW, WZ, SZ, YXX, YBJ and PY, performed the work described here. RKT, QP, JGF, ARH and TVL provided the human samples and performed histopathological work. LZ, YXC and XZR designed the study. LZ, ZV, JFM, MP, YXC and XZR wrote the manuscript.

Word Count: 5941

Numbers of Figures: 8

**Abstract**

**Background and Aims:** Fatty acid translocase CD36 (CD36) is a membrane protein with multiple immuno-metabolic functions. Palmitoylation has been suggested to regulate the distribution and functions of CD36, but little is known about its significance in NASH.

**Methods:** Human liver tissue samples were obtained from patients undergoing liver biopsy for diagnostic purposes. CD36 knockout mice were injected with lentivirus vectors to express wild type CD36 and palmitoylation sites mutated CD36 in the livers. Liver histology, immunofluorescence, mRNA expression profile, subcellular distributions and functions of CD36 protein were assessed.

**Results:** The localization of CD36 on the plasma membrane of hepatocytes was markedly increased in patients with NASH compared to patients with normal liver and those with simple steatosis. Increased CD36 palmitoylation and increased localization of CD36 on the plasma membrane of hepatocytes were also observed in livers of mice with NASH. Furthermore, inhibition of CD36 palmitoylation protected mice from developing NASH. The absence of palmitoylation decreased CD36 protein hydrophobicity reducing its localization on the plasma membrane as well as in lipid raft of hepatocytes. Consequently, a lack of palmitoylation decreased fatty acid uptake and CD36/Fyn/Lyn complex in HepG2 cells. Inhibition of CD36 palmitoylation not only ameliorated intracellular lipid accumulation via activating the AMPK pathway, but also inhibited inflammatory response through the inhibition of the JNK signaling pathway.

**Conclusions:** Our findings demonstrate the key role of palmitoylation in regulating CD36 distributions and its functions in NASH. Inhibition of CD36 palmitoylation may represent an effective therapeutic strategy in patients with NASH.

## Lay summary

Fatty acid translocase CD36 (CD36) is a multifunctional membrane protein which contributes to the development of liver steatosis. In the present study, we demonstrated that the localization of CD36 on the plasma membrane of hepatocytes is increased in patients with NASH. Blocking the palmitoylation of CD36 reduces CD36 distribution in hepatocytes plasma membrane and protects mice from NASH. The inhibition of CD36 palmitoylation not only improved fatty acid metabolic disorders but also reduced the inflammatory response in vitro and in vivo. The present study suggests that CD36 palmitoylation is important for NASH development and inhibition of CD36 palmitoylation could be used to cure NASH.

## Introduction

Non-alcoholic fatty liver disease (NAFLD) describes a range of conditions caused by the accumulation of fat in hepatocytes. Fifteen percent to 30% of the general population in both the Western world and Asia suffer from NAFLD [1, 2]. The prevalence is increased in type 2 diabetes mellitus (T2DM) (70%) and morbid obesity (90%) [3]. Non-alcoholic steatohepatitis (NASH) is a subset of NAFLD characterized by excessive fat accumulation in hepatocytes (steatosis) associated with liver tissue inflammation. Unlike steatosis alone (simple steatosis, SS), which is generally considered benign and reversible, NASH may progress to fibrosis, cirrhosis and hepatocellular carcinoma [4, 5]. Approximately 2-3% of the global population is supposed to have NASH, tending to rise rapidly along with incidence of obesity, T2DM and the metabolic syndrome [6, 7]. The pathogenesis of NASH appears complex and it is still poorly understood, hence there are no specific therapeutic strategies for NASH.

Fatty acid translocase CD36 (CD36) is a widely expressed membrane glycoprotein, which plays an important role in facilitating the uptake and intracellular trafficking of long-chain fatty acid (LCFA) [8, 9]. Growing evidence indicates that the role played by CD36 extends far beyond the transport of fatty acids (FA). Indeed, CD36 also impacts FA oxidation by influencing the activation of monophosphate-activated protein kinase (AMPK) [10]. More importantly, CD36 is engaged in the regulation of chronic metabolic inflammation. Stewart et al. reported that CD36 ligands (oxidized LDL and amyloid-beta) are able to trigger inflammatory signaling through the assembly of a complex of CD36 and toll-like receptors 4/6 [11, 12]. CD36 deletion markedly reduced adipocyte inflammation in mice fed with a high-fat diet (HFD) by inhibiting the JNK pathway [13]. Accordingly, CD36 has been recognized as a multifunctional immuno-metabolic receptor [14].

Hepatic CD36 expression is normally weak, but its expression is significantly increased in animal models and patients with steatosis [15, 16]. Hepatic overexpression (OE) of CD36 results in steatosis in mice even in the absence of a high-fat diet (HFD) [17], and liver-specific knockout (KO) of CD36 reduces liver

lipid content when mice were fed with HFD [18]. However, little is known about the role of CD36 in NASH.

It is well-established that CD36 functions are largely dependent on its localization on the plasma membrane [19]. Insulin and the forkhead transcription factor FoxO1 induce CD36 translocation from intracellular depots to the plasma membrane, facilitating FA uptake [20]. However, the mechanisms regulating CD36 localization on the plasma membrane remain poorly understood.

Palmitoylation is the covalent attachment of palmitate to cysteine residues of proteins. This post-translational modification increases the lipophilicity of the modified protein, thus regulating its subcellular distribution and function [21]. It has been confirmed that human CD36 is palmitoylated, cysteine residues (cys) 3, 7, 464, and 466 account for the entire palmitoylation of CD36 [22]. Inhibition of palmitoylation causes ER accumulation of CD36 and decreases its incorporation into plasma membrane rafts, thus reducing the efficiency of uptake of oxidized low density lipoprotein in melanoma cell lines [23].

The functional consequences of palmitoylation of CD36 within the liver and its role in NASH have never been addressed. In the present study, we demonstrated that the localization of CD36 on the plasma membrane of hepatocytes was significantly increased in patients with NASH and we provide detailed mechanistic insights on the role of CD36 palmitoylation in the pathogenesis of NASH in a HFD-induced NASH mice model. The results of the study suggest that CD36 palmitoylation represents a pathogenic link between FA metabolic dysfunction and liver tissue inflammation in NASH.

## Materials and Methods

**Human samples.** The study included 79 non-diabetic liver tissue biopsy samples obtained from the Affiliated Hospital of Chongqing Medical University (CQMU) (9 patients) and Xinhua Hospital of Shanghai Jiaotong University School of Medicine (SJTUSM) (10 patients), China and from the Royal Free Hospital (60 patients), United Kingdom. The liver samples were obtained either by liver biopsy

for diagnostic purpose or from surgical liver resections. All patients provided written informed consent for their tissue to be analyzed for research purposes. The study was approved by the Hospital Ethics Committees of CQMU, SJTUSM and the Royal Free Hospital. Main inclusion criteria were daily alcohol consumption <20 g, negative tests for viral infections (hepatitis B virus, hepatitis C virus and human immunodeficiency virus) or other causes of acute or chronic liver diseases. Tissue sections were reviewed by liver pathologists in Chongqing Medical University and the Royal Free Hospital, and classified/subdivided into four groups: normal liver (NL, n=20), simple steatosis (SS, n=19), NASH (n=21) and cirrhosis (n=19).

**Histology, ORO, sirius red staining.** Paraffin-embedded tissue sections were routinely stained with hematoxylin and eosin (HE) using standard protocols. Staining with Sirius red was performed for visualizing liver tissue fibrosis. For Sirius red staining, sections were stained for 90 min with Direct Red 80 dye (Sigma Aldrich). All images were captured using a Zeiss microscope. Image analysis procedures were performed with Image J software. The percentage of liver tissue area occupied by fatty hepatocytes or Sirius red-positive area was obtained from six different fields in each sample. The average values were considered as hepatic steatosis index and fibrosis index.

**Plasmid, lentivirus production and stable cell lines.** The mammalian expression plasmid PCI-CD36 encoding wild type human CD36 full-length cDNA was kindly provided by Kenneth J. Linton (Queen Mary, University of London). A CD36 variant was generated using PCI-CD36 as a template and the mutation primers (Supplementary table 1) with a multiple site-directed mutagenesis Kit (QuickChange II XL, Agilent Technologies), in which the cysteine pair (Cys-3, 7) of wild type CD36 were replaced with alanine, and the residues towards the carboxyl terminus (Cys-464, 466) were replaced with serine (Supplementary Figure 2A). The lentivirus constructs including GV341 empty vector (NC-vector), GV341 containing wild type CD36 (wt-CD36), AA-SS mutant (AA-SS CD36) were provided by Shanghai GeneChem Company. HepG2 cells were infected with a

multiplicity of infection (MOI) of 10 and stable transfectants were selected with puromycin (Shanghai Sangon) and named as NC-HepG2, wt-CD36-HepG2, and AA-SS-HepG2, respectively.

**Experimental animals.** 8-week-old male C57BL/6J mice were fed with a high fat diet (HFD), (n=6) or normal chow diet (NCD) (n=6) for 22 weeks (research diets 12492, 12109B). In some experiments, the 8-week-old male CD36 knockout (CD36KO) mice were injected with NC lentivirus vectors (n=6), wt-CD36 lentivirus vectors (n=6) and AA-SS lentivirus vectors (n=6) in the tail vein and kept on HFD for 8 weeks. All mice were housed in a temperature-controlled environment and 12 h, 12 h light: dark cycle with free access to diet and water. Before sacrifice, mice were fasted overnight. The animal treatment conformed to the guidelines of The Institutional Animal Care and Use Committee of Chongqing Medical University. Before sacrifice, mice were deprived of food overnight with free access to water. The contents of free fatty acid (FFA) in mice serum were analyzed by an automatic biochemistry analyzer. All mouse care and experimental procedures were previously approved by the Institutional Animal Care and Use Committee of Chongqing Medical University, and the investigation conforms with the Guidelines for the Care and Use of Laboratory Animals published by the US National Institutes of Health (NIH Publication No. 85-23, revised 1996).

**Lipid droplet staining and measurement of fluorescent signals.** For lipid droplet staining, cells were fixed with paraformaldehyde and stained with 400 $\mu$ M Bodipy493/503 for 30 min. All images were captured using a Zeiss microscope. A fluorescent counter was also used to measure the relative fluorescent units (RFU) of lipid droplet staining.

**Immunofluorescent staining and confocal microscopy.** Paraffin-embedded tissue sections were incubated with anti-CD36 (Novus) and anti-beta catenin (Abcam) followed by an incubation of FITC-labeled anti-rabbit IgG and TRITC-labeled anti-mouse IgG. Then sections were stained with DAPI and images were captured using a Leica confocal microscope. The Pearson's correlation (R value) and co-localization rate were analyzed from four different

fields in each sample using Leica confocal microscope software.

**Quantitative analysis of hepatic triglyceride (TG).** Hepatic lipids were extracted from livers using a mixture of chloroform and methanol. The contents of hepatic TG were measured by a commercial Kit (Nanjing Jiancheng Bioengineering) and normalized by tissue weight.

**Analysis of mRNA expression.** Total RNA was reverse transcribed using MultiScribe reverse transcriptase (Applied Biosystems). cDNA (25 ng) was used with 0.25 $\mu$ M target (tumor necrosis factor alpha [TNF $\alpha$ ], interleukin 6 [IL-6], monocyte chemoattractant protein 1 [MCP-1], collagen I [Coll], transforming growth factor beta [TGF $\beta$ ] or control (36B4) oligonucleotide primers (Supplementary table 2). Quantitative RT-PCR was performed using a CFX Real-Time PCR Detection System (Bio-Rad). Relative mRNA expression was calculated using the comparative cycle method ( $\Delta\Delta$ Ct).

**Western blots and co-immunoprecipitations.** Tissues extracts and cells were lysed using radioimmuno-precipitation (RIPA) buffer. For Western blotting analysis, equal amounts of protein were subjected to sodium dodecyl sulfate–polyacrylamide gel electrophoresis (SDS-PAGE) and electrotransferred to PVDF membranes (Millipore). Membranes were incubated with primary antibodies, subsequently being incubated with HRP-conjugated secondary antibodies. For immunoprecipitation (IP), equal amounts of lysate proteins were incubated (4 $^{\circ}$ C) with antibodies overnight before adding protein A/G magnetic beads (Millipore) (1–3 h). Bound proteins were eluted by boiling for 5 min in SDS sample buffer, and cleared supernatants were resolved by SDS-PAGE. Detection was performed with the Protein Detection System (Fusion FX5) and ECL Plus reagent (Amersham). The band intensity was analyzed by densitometry software (Image J).

**Detection of CD36 protein palmitoylation.** Protein palmitoylation was assessed by immunoprecipitation and acyl-biotin exchange (IP-ABE) as previously described [24]. Briefly, total protein was extracted using a lysis buffer with protease inhibitors and N-ethylmaleimide (NEM). After precipitating CD36 protein with anti-CD36body (Novus) and magnetic beads (Millipore), samples were

re-suspended with stringent buffer. Added 0.5 ml/sample of lysis buffer pH 7.2 to all - hydroxylamine (HAM) samples, and 0.5 ml/ sample of HAM buffer to all +HAM samples. All samples were rotated at room temperature for 50min. Then samples were added with Biotin-BMCC buffer, and rotated for 50min at 4°C. Proteins were eluted from the beads by boiling in sample buffer and the cleared supernatants were resolved by SDS-PAGE and electro-transferred to PVDF membranes (Millipore). For detecting palmitoylated CD36, membranes were incubated with HRP-conjugated anti-streptavidin for 1 hour at 37°C. For detecting total CD36, membranes were incubated with anti-CD36 (Novus) and subsequent HRP-conjugated secondary antibody (Zsbio).

**NF- $\kappa$ B activity assay.** Cells were transfected with an NF- $\kappa$ B response element-luciferase reporter gene and reporter gene activity was measured using the Dual Luciferase Assay Reporter System (Promega) as previously described [11].

**Bioinformatic analysis.** Palmitate is a LCFA with 16-carbons atom and with little of polar atom, so palmitoylation can be estimated as 4 Lysines replaced on the original cysteine residues (palmitoylated and non-palmitoylated CD36 amino sequences are listed in the supplementary table 3). The 36 amino acids of protein N-terminal and C-terminal is predicted by the method of tree threader calculation (<http://protein.ict.ac.cn/TreeThreader/>, Bioinformatics lab, Institute of Computing Technology, Chinese Academy of Sciences). The protein hydrophobic and hydrophilic model is shown by Chimera (<http://www.cgl.ucsf.edu/chimera/>). The hydrophobic and hydrophilic regions are red and blue respectively. The hydropathy values of amino acids in wt-CD36 and AA-SS CD36 were acquired using online software (<http://web.expasy.org/protparam/>). The grand average of hydropathicity (GRAVY) of wt-CD36 and AA-SS CD36 was calculated as the sum of hydropathy values of all amino acids divided by the numbers of residues in the sequence. The accessible molecular surface was calculated using the 'What If program' (<http://swift.cmbi.ru.nl/servers/html/index.html>).

**Isolation and analysis of cellular plasma membrane fractions.** The cellular plasma membrane was isolated using a commercial Kit (Abcam) according to the manufacturer's instruction. Briefly, cells (wet weight about 0.2-1g) were collected and homogenized in Homogenize Buffer Mix. The homogenate was then centrifuged at 700 x g for 10 minutes to remove the nuclear pellet. The supernatant from the original 700 x g spin was centrifuged at 10000 x g for 30 min at 4 °C. The supernatant was collected and designated "cytoplasm extracts". The pellet was re-suspended in Upper and Lower Phase solution to separate plasma membrane fractions from cellular organelle membrane. The suspension was mixed thoroughly and centrifuged at 1000 x g for 10 min at 4 °C. Upper Phase solution was collected and diluted it with 5 volumes of water. Then the mixture was centrifuged at 14000 x g at 4 °C for 20 minutes. The plasma membrane fraction pellet was dissolved in 0.5% Triton X-100.

**Isolation and analysis of detergent-resistant membranes (DRMs).** Plasma membrane lipid rafts were identified as DRMs and were obtained by floatation on sucrose density gradients by ultracentrifugation of Triton X-100 lysates as previously described [25]. The partitioning of CD36 to the DRM and non-DRMs fractions was determined using Image J software.

**Flow cytometry.** Cells were fixed and permeabilized with 0.1% saponin prior to labeling by direct immunofluorescence using PE-conjugated CD36 antibody (Millipore). Then cellular CD36 expression was examined by a FACScan flow cytometer (Becton-Dickinson).

**Bivariate analysis of LCFA binding or uptake.** FL labeled palmitate (FL-C16, Invitrogen) was incubated with the HepG2 cells for 2 hours (4 °C for LCFA binding and 37 °C for LCFA uptake). Then cells were immuno-stained with anti-CD36-PE (Millipore) before data acquisition using a FACScan flow cytometer. The data were exported and analyzed using a previously reported bivariate spreadsheet method [26] with some modification. Briefly, all cell event data were categorized according to the levels of expression of CD36 in SPSS software. After excluding channels below three cell events, the mean and standard deviates of

fluorescence values for ligand (FL-C16) were calculated for each receptor (CD36) level category. Then these data were exported into EXCEL2007 and a Student's t-test was performed to compare the binding/uptake of ligand for receptor categories displaying equivalent receptor expression between two groups. The average of FL-C16 uptake vs. CD36 expression and statistical results were plotted using EXCEL.

**Measurements of O<sub>2</sub> consumption.** A Seahorse Bioscience XF24 instrument was used to measure the rate of change of dissolved O<sub>2</sub> in medium immediately surrounding cells cultured in 24-well plates. The rates of O<sub>2</sub> concentration were obtained from the slopes of concentration changes versus time measured during serial 180-second plunge periods that were followed by 180-second mix and 120-second wait periods. Various metabolic inhibitors (oligomycin, FCCP and R/A) were added via automatic injectors followed by periods of 180 s of mixing, 120 s of waiting and 180s of measuring. The capabilities of cellular fatty acid oxidation (FAO) were measured by the difference between O<sub>2</sub> consumption with and without palmitate substrates.

**Statistic analysis.** The difference between two groups was statistically analyzed by Student's t-test. The differences among three or more groups were statistically analyzed by analysis of variance (one-way ANOVA) with Tukey's multiple comparisons test. A P-value of <0.05 was considered significant.

**Study approval.** All mouse care and experimental procedures were previously approved by the Institutional Animal Care and Use Committee of Chongqing Medical University, and the investigation conforms with the Guidelines for the Care and Use of Laboratory Animals published by the US National Institutes of Health (NIH Publication No. 85-23, revised 1996).

## Results

**CD36 localization on the hepatocellular plasma membrane is significantly increased in patients with NASH.** Compared with the NL group, evident lipid droplets were observed in livers of the patients with SS (Figure 1Aii),

while steatosis was associated with evident inflammatory cell infiltration in liver sections from patients with NASH (Figure 1A iii). A hepatic steatosis index was evaluated by measuring the percentage of the liver tissue area occupied by fatty hepatocytes, as described in Methods. As shown in Figure 1B, the hepatic steatosis index was similar in patients with SS and NASH and was significantly higher than in NL and cirrhotic patients. On the other hand, both Sirius red staining and the hepatic fibrosis index were significantly higher in patients with NASH and cirrhosis (Figure 1C and 1D).

As  $\beta$ -catenin is localized on the hepatocyte plasma membrane, we next investigated CD36 distribution on the plasma membrane of hepatocytes in samples of normal liver (NL) as well as from patients with different stages of NAFLD (SS, NASH and cirrhosis), using a dual-staining of CD36 and  $\beta$ -catenin. The CD36 expression was weak in the liver samples from NL subjects (Figure 1E v), but it was increased in the patients with SS (Figure 1E vi) and NASH (Figure 1E vii), and became weak again in cirrhotic patients (Figure 1E viii). More importantly, the localization of CD36 on hepatocytes plasma membrane was significantly increased in NASH patients (Figure 1E xi and xv). We further quantified the colocalization efficiency of CD36 and  $\beta$ -catenin in this group of patients. As shown in Figure 1F, the Pearson's correlation (R value of CD36 and  $\beta$ -catenin staining) was higher in patients with SS than in those with NL and was highest in NASH patients, suggesting that the localization of CD36 on the plasma membrane of hepatocytes is positively correlated with the evolution from NL to SS and to NASH. Notably, the R value was lower in cirrhosis than with NASH, which may be due to massive loss of hepatocytes in cirrhotic livers (Figure 1F). The co-localization rate was also significantly increased in the patients with NASH compared with subjects with NL or SS or cirrhosis (Figure 1G). These findings further support that CD36 localization on the plasma membrane of hepatocytes is associated with the development of NASH.

**CD36 palmitoylation is induced in the liver of mice with NASH.** Since palmitoylation is closely related to the translocation of membrane protein from an

intracellular pool to the plasma membrane, we investigated the role of hepatic CD36 expression and palmitoylation in a mice model of NASH. As shown in Figure 2A, after 22 weeks of feeding with a high fat diet (HFD), C57BL/6J mice developed a typical hepatocellular ballooning (Figure 2A ii, iv), lobular inflammation (Figure 2A ii) and moderate fibrosis (Figure 2A vi). Hepatic steatosis and fibrosis indexes and TNF $\alpha$  expression were all significantly increased in livers of mice with HFD (Figure 2B and 2C). Thus, long-term HFD feeding induced NASH in C57BL/6J mice. Western blot analysis demonstrated that CD36 protein levels were higher in the livers of mice with NASH when compared to NCD (Figure 2D). Next we analyzed the localization of CD36 on the plasma membrane of mouse hepatocytes. Hepatic CD36 expression was more evident in mice with NASH (Figure 2E iv) than in mice with normal livers (Figure 2E iii). The co-localization of CD36 and  $\beta$ -catenin was also significantly increased in mice with NASH (Figure 2E, 2F), in agreement with our finding in patients with NASH.

The palmitoylation of hepatic CD36 in HFD mice versus NCD mice was then further investigated by immunoprecipitation and acyl-biotin exchange (IP-ABE) method (Figure 2G). The results of IP-ABE indicated that palmitoylated CD36 protein was significantly increased in the livers of mice with NASH when compared to NCD mice.

In HepG2 cells, palmitic acid (PA) dose-dependently increased mRNA levels of CD36 (supplementary Figure 1A). PA also promoted the palmitoylation of CD36 in HepG2 cells (supplementary Figure 1B). In addition, the FFA contents in serum were significantly increased in mice with HFD than in mice with NCD (supplementary Figure 1C), suggesting that PA, which is the most abundant FFA in hyperlipidemic serum, contribute to the increased palmitoylation of CD36 in the liver.

**Inhibition of CD36 palmitoylation protects mice from NASH.** To further identify the role of CD36 palmitoylation in NASH, we constructed lentivirus vectors expressing wt-CD36 and AA-SS CD36 and validated them in cells. CD36 expression was increased in both wt-CD36-HepG2 and AA-SS-HepG2 cells

(Supplementary Figure 2B). Palmitoylated CD36 levels were significantly higher in wt-CD36-HepG2 cells than in NC-HepG2 cells. In contrast, the levels of palmitoylated CD36 to total CD36 in AA-SS-HepG2 cells were almost equal to NC-HepG2 cells (Supplementary Figure 2C).

Next, we injected CD36KO mice with lentivirus vectors to express wt-CD36 and AA-SS CD36. As endogenous CD36 was absent in this model, its effects were excluded. As shown in Figure 3A, CD36 protein was absent in the livers of CD36KO mice, while it was significantly increased in hepatocytes of CD36KO-wt CD36 and CD36KO-AA SS mice (Figure 3A iv, v, vi). These findings were consistent with the results from Western blotting of CD36 in mice livers (supplementary Figure 2D). The distribution of CD36 on hepatocyte plasma membranes was more evident in wt-CD36 OE mice livers (Figure 3A xi) than in NC (Figure 3A x) and in AA-SS CD36 OE mice livers (Figure 3A xii). As CD36 was absent in the NC group, the Pearson's correlation and co-localization rate were lowest in the NC group compared to the wt-CD36 and AA-SS groups (Figure 3B and 3C). The Pearson's correlation and co-localization rate were higher in the wt-CD36 group than in the AA-SS groups.

When compared with CD36KO-NC mice, evident inflammatory cells infiltration (Figure 3D ii), more abundant lipid droplets (Figure 3D, v) and mild tissue fibrosis (Figure 3D viii) were observed in the livers of CD36KO-wt CD36 mice. Interestingly, hepatic steatosis with inflammation and fibrosis were decreased in the CD36KO-AA SS mice, compared with CD36KO-wt CD36 mice (Figure 3D iii, vi, ix). The TG quantitative data also showed that hepatic content of TG in CD36KO-wt CD36 mice was significantly higher than in CD36KO-NC and CD36KO-AA SS mice (Figure 3E). The hepatic mRNA levels of cytokines/chemokine (TNF $\alpha$ , IL-6 and MCP-1) and fibrosis markers (collagen IV and TGF $\beta$ ) were significantly increased in CD36KO-wt CD36 mice, whereas the expression of these genes was significantly reduced in the CD36KO-AA SS mice (Figure 3F and 3G). These findings clearly demonstrated that CD36 palmitoylation represents a mechanistic step in the development of NASH.

**Inhibition of CD36 palmitoylation influences protein hydrophobicity and its localization on the hepatocellular plasma membrane.** Based on the observation that inhibition of palmitoylation reduced the development of NASH, we next investigated the possible underlying mechanisms. Using bio-informatics, we predicted the N-terminal and C-terminal 3D protein structures of palmitoylated CD36 and non-palmitoylated CD36. As shown in the Supplementary Figure 3, the conformation of palmitoylated CD36 was clearly different from non-palmitoylated CD36. We also calculated the hydrophobic values of wt-CD36 (blue) and AA-SS CD36 protein (red) by the Kyte-Doolittle method (Figure 4A). The Grand Average of Hydrophobicity (GRAVY) was calculated as the sum of hydrophobicity values of all amino acids divided by the numbers of residues in the sequence. An increasing positive score indicates greater hydrophobicity. The GRAVY in wt-CD36 was 0.122 in comparison with 0.022 in AA-SS CD36 (Figure 4B), suggesting that wt-CD36 has stronger hydrophobicity than AA-SS CD36. Calculation of the accessible surface area confirmed that wt-CD36 had a much less hydrophobic surface area than AA-SS CD36 (Figure 4C). Thus inhibition of palmitoylation increases hydrophobicity of CD36, which may decrease the affinity of CD36 to the plasma membrane thus hindering CD36 translocation from intracellular pools to the cell membrane [27].

Next, we isolated the subcellular fractions to confirm the effects of palmitoylation on CD36 distribution on cell plasma membrane. Flow cytometry results showed that total CD36 expression were significantly increased in wt-CD36-HepG2 and AA-SS-HepG2 cells compared to NC-HepG2 cells, and its expression was roughly equal in wt-CD36-HepG2 and AA-SS-HepG2 cells (Figure 4D). Furthermore, as shown in Figure 4E, a weaker CD36 plasma membrane signal contrasted with a stronger CD36 cytoplasm signal in AA-SS-HepG2, as compared to wt-CD36-HepG2 cells.

Given that the plasma lipid raft is an essential domain for CD36-mediated FA uptake [28], we further investigated the impact of inhibition of CD36 palmitoylation on its distribution in the lipid rafts of HepG2 cells. DRM analysis revealed that

CD36 from the wt-CD36-HepG2 was highly enriched within the visible floating band that also contained caveolin, a lipid raft marker, while CD36 in the AA-SS-HepG2 cells was less evident within the DRM fractions (Figure 4F). This pattern of distribution was confirmed to be statistically significant and consistent in different preparations (Figure 4F).

**Inhibition of CD36 palmitoylation reduces long-chain fatty acid (LCFA) binding/uptake and CD36/Fyn/Lyn complex formation in HepG2 cells.** As studies have identified CD36 as a key mediator of LCFA uptake [8, 9], we next investigated whether the absence of CD36 palmitoylation inhibited LCFA binding or uptake in HepG2 cells. A bivariate flow cytometric assay, a technique developed to overcome the bias of differences in receptor expression in cell based ligand binding/uptake assays, was applied to quantitatively examine the binding and uptake of LCFA in cells. There was a significant decrease in the binding and uptake of LCFA, as reported by the fluorescent lipid analogue (FL-C16), in the AA-SS-HepG2 relative to the wt-CD36-HepG2 cells (Figure 5A, 5B). 2BP decreased LCFA binding and uptake in HepG2 cells (Figure 5C, 5D).

CD36 not only functions as a FA transporter but it also recruits the src family kinase Fyn and Lyn to assembly signaling protein complexes [10]. We examined whether palmitoylation was involved in modulating CD36 association with Fyn and Lyn. AA-SS mutation markedly decreased the amounts of Fyn and Lyn found in CD36 IP from OE HepG2 cells (Figure 5E), suggesting a reduced CD36-Fyn/Lyn association. These data support the hypothesis that inhibition of CD36 palmitoylation suppresses the formation of CD36/Fyn/Lyn complex.

**Inhibition of CD36 palmitoylation enhances FA  $\beta$ -oxidation by activating the AMPK pathway.** In patients with NAFLD, FA  $\beta$ -oxidation in hepatocytes is significantly decreased, contributing to the abnormal lipid accumulation. Along these lines, we measured FA-driven oxygen consumption rate (palmitate-dependent OCR) to assess the effects of CD36 palmitoylation on FA  $\beta$ -oxidation (FAO). As shown in Figure 6A, the wt-CD36-HepG2 cells always had lower palmitate-dependent oxygen consumption versus the NC-HepG2 cells. The

AA-SS-HepG2 cells had always higher palmitate-dependent oxygen consumption versus wt-CD36-HepG2 cells, indicating the improved FAO in the former (Figure 6B). We also observed a markedly increase of FAO in HepG2 treated with 2-bromopalmitate (2-BP) when compared with cells without 2-BP (Figure 6C). Thus inhibition of CD36 palmitoylation in hepatocytes clearly correlated with the increased FAO.

AMPK is a key regulator in the maintenance of cellular FA homeostasis [29], which controls FA  $\beta$ -oxidation in mitochondria. As shown in Figure 6D, phosphorylation of AMPK was lower in the wt-CD36-HepG2 cells than in the NC-HepG2 cells, suggesting that CD36 overexpression inactivated the AMPK pathway. Interestingly, the absence of CD36 palmitoylation increased phosphorylation of AMPK compared with wt-CD36 HepG2 cells (Figure 6D). 2-BP, an inhibitor of palmitoylation also increased the phosphorylation of AMPK in HepG2 cells (Figure 6E). These findings suggested that inhibition of CD36 palmitoylation results in the activation of the AMPK pathway.

Furthermore, compound C, an inhibitor of AMPK, was applied to test whether the activation of AMPK contributed to the enhanced FAO in AA-SS-HepG2 cells. Both basal FAO (palmitate-dependent OCR before oligomycin treatment) and max FAO (palmitate-dependent OCR in response to uncoupling agent, FCCP) were significantly decreased in compound C-treated AA-SS-HepG2 cells, as compared with untreated cells (Figure 6F). Moreover, we found that, while in the absence of compound C, lipid accumulation is less evident in AA-SS-HepG2 than in wt-CD36-HepG2 cells; the amount of lipid droplets became equally evident in wt-CD36-HepG2 and in AA-SS-HepG2 cells in the presence of compound C (Figure 6G). We also tested the effects of compound C on 2BP-treated HepG2 cells. As shown in Figures 6H and 6I, in the absence of compound C, 2BP significantly inhibited palmitate-induced lipid droplets accumulation. However, in the presence of compound C, the numbers of lipid droplets in 2BP-treated cells were significantly increased reaching equal levels of palmitate-treated HepG2 cells. Thus inhibition of CD36 palmitoylation enhanced FAO via activation of AMPK,

resulting in reduced intracellular lipid accumulation in hepatocytes.

**Inhibition of palmitoylation reduces inflammation via inhibiting the JNK pathway.** CD36 not only regulates FA metabolism, but also modulates the inflammatory response. While the NF- $\kappa$ B activities were higher in the wt-CD36-HepG2 than in the NC-HepG2 cells, there was no difference between AA-SS-HepG2 and NC-HepG2 cells (Figure 7A). TNF $\alpha$  protein levels were consistently higher in wt-CD36-HepG2 than in NC-HepG2 cells; TNF $\alpha$  expression was significantly lower in the AA-SS-HepG2 than in wt-CD36-HepG2 cells (Figure 7B). TNF $\alpha$  expression was also reduced in 2BP-treated HepG2 cells (Figure 7C). These findings demonstrated that CD36 palmitoylation plays an important role in mediating the inflammatory response.

The c-Jun NH(2)-terminal kinase (JNK) contributes to steatohepatitis and fibrosis [30]. Following treatment with SP600125, an inhibitor of JNK signaling pathway, TNF $\alpha$  expression was not increased in the wt-CD36-HepG2 cells (Figure 7D). Thus JNK signaling pathway is a critical determinant of CD36-mediated inflammatory response.

We next examined whether the palmitoylation of CD36 influenced the activation of JNK signaling pathway. Phosphorylated JNK was significantly increased in wt-CD36-HepG2 compared to NC-HepG2 cells and AA-SS mutation markedly decreased the amounts of phosphorylated JNK as compared with wt-CD36-HepG2 cells (Figure 7E). The reduced phosphorylation of JNK was also observed in 2-BP-treated HepG2 cells (Figure 7F). Thus inhibition of CD36 palmitoylation inactivated JNK signaling pathway, reducing liver tissue inflammation.

## Discussion

Lipid accumulation and tissue inflammation are key features of NASH. However, the pathogenic cross-roads linking FA metabolism, lipotoxicity and hepatic inflammation/fibrogenesis remain unclear. CD36 is a widely expressed membrane glycoprotein playing an important role in modulating FA uptake and FA

$\beta$ -oxidation, contributing to the maintenance of cellular FA homeostasis [10, 31]. In addition, CD36 regulates a downstream pathway modulating NF- $\kappa$ B activity which activates cellular inflammatory response [11, 12]. In these terms, CD36 represents a crucial link between FA metabolic dysregulation and inflammation, which synergistically contributes to the development of NASH.

Previously, the potential role of CD36 in the pathogenesis of human NAFLD was suggested by the study of Miquilena-Colina et al., showing that CD36 is overexpressed and associated with insulin resistance, hyperinsulinemia and increased steatosis in patients with NAFLD and HCV with fatty liver [32]. In the present study, we confirmed that CD36 expression increased with evolution from normal liver to SS and further development to NASH. Since CD36 is widely expressed in many cell types, including monocytes, macrophages and hepatocytes [33], we characterized CD36 distribution on the hepatocellular plasma membrane using co-immunofluorescent staining of CD36 and  $\beta$ -catenin, a hepatocyte plasma membranes marker. Our results show that the distribution of CD36 on the plasma membrane of hepatocytes is remarkably increased in patients with NASH compared with those with SS and cirrhosis, suggesting that the increased localization of CD36 on hepatocyte plasma membranes may represent a key feature in the development of NASH.

The evident plasma membrane localization of CD36 found in patients with NASH prompted the investigation of the possible mechanism(s) regulating the distribution of this protein. Previous studies demonstrated that insulin increases CD36 palmitoylation and rapidly stimulates the surface expression of CD36 in muscle cells [34, 35]. In addition, Thorne et al. consistently found that palmitoylation is necessary for the efficient incorporation of CD36 into plasma membrane rafts in melanoma cells [23]. Therefore, the role of CD36 palmitoylation in the development of NASH was investigated in the present study. We examined the levels of palmitoylation of CD36 in livers of mice with NASH. Hepatic palmitoylated CD36 was significantly increased in mice with NASH, with demonstrable hepatocyte plasma membranes expression, in agreement with the

findings obtained in patients with NASH. It is conceivable that palmitoylation enhances the hydrophobicity of CD36, thus increasing its distribution in hepatocellular plasma membrane rafts, a special lipid-rich plasma membrane microdomains facilitating FA take and interactions between proteins [19, 21, 27, 36].

Consequently, the palmitoylated CD36 on the hepatic plasma membrane mediates FA uptake and enhances the formation of the CD36/Lyn/Fyn complex with the consequent activation of an inflammatory cascade, which distinguishes NASH from SS. Accordingly, inhibition of CD36 palmitoylation leads to the inactivation of the NF- $\kappa$ B signaling pathway, followed by reduced inflammatory reaction both *in vivo* and *in vitro*. JNK plays an important role in the development of NASH. Deletion of JNK diminishes hepatic inflammation induced by a high-fat diet and a methionine- and choline-deficient (MCD) diet respectively in mice, [37, 38]. The activation of JNK in response to multiple stresses mediates inflammation through activator protein-1–dependent transcription of proinflammatory cytokines [30]. CD36 recruits the src kinase Lyn, which phosphorylates and activates JNK, contributing to adipose tissues inflammation [39]. The interaction between CD36 and src kinase Lyn required the MISY motif on 460-463 amino acids residues of C-terminus of CD36 [11], which is near by the palmitoylation sites on the C-terminus of CD36 (residues 464 and 466). In this study, we show that the absence of CD36 palmitoylation significantly decrease the interaction between CD36 and Lyn, resulting in reduced JNK activation and inflammatory responses. Since inflammatory stress affects multiple steps in FA metabolisms, resulting in hepatic steatosis [40], the attenuated inflammation may also contribute to the reduced lipid accumulation in the liver.

Interestingly, inhibition of CD36 palmitoylation, either by mutations of palmitoylation sites (AA-SS) of CD36 or pharmacological agent, inhibited FA binding, uptake and an inflammatory response. In the present study, the specific role of CD36 palmitoylation was identified by the mutation on CD36 palmitoylation sites. Wild type CD36 (wt-CD36) overexpression caused steatosis and

inflammation in mice livers, while mice bearing the palmitoylation-sites mutated CD36 (AA-SS) did not develop NASH. 2-BP, which is not a specific inhibitor of CD36 palmitoylation although they have been widely used to test the general role of palmitoylation of protein [23], prevented the development of hepatic steatosis. Accordingly, more specific inhibitors of CD36 palmitoylation should be considered in future studies for the treatment/prevention of NASH.

The excess of lipids in hepatic steatosis is mainly constituted by TG, which are stored in cytoplasmic lipid droplets [41]. Excessive influx of FA from the circulation to the liver is normally handled by FA  $\beta$ -oxidation. However, lipid overload particularly in the presence of tissue inflammation leads to the impairment of FA  $\beta$ -oxidation, as shown in this study, and leads to the worsening of steatosis. AMPK plays an important role in maintaining energy homeostasis and may have therapeutic importance for treating obesity, insulin resistance, type 2 diabetes, cardiovascular disease and hepatic steatosis [42]. AMPK is normally quiescent, and it is phosphorylated and activated in response to energy stresses, leading to a decrease in ATP-consuming pathways and an increase in ATP-producing pathways. Liver-specific activation of AMPK completely protects mice against high-fructose diet-induced hepatic steatosis [43]. Hepatic activation of AMPK has been reported to promote FAO via phosphorylation and inactivation of ACC, reducing levels of the  $\beta$ -oxidation inhibitor malonyl-CoA [44]. Previous studies have demonstrated that CD36 is presented in a protein complex with the AMPK kinase LKB1 (liver kinase B1) and the src kinase Fyn [10]. Wt-CD36 overexpression promotes Fyn mediated LKB1 phosphorylation and its nuclear sequestration, hindering LKB1 mediated phosphorylation and activation of AMPK [45]. Consistent with this, we found that palmitoylation of CD36 is associated with a low AMPK activity, accompanying a low hepatic FA  $\beta$ -oxidation, which may also due to the increased LKB1 phosphorylation, a negative regulator of AMPK. On the other hand, AMPK phosphorylation was enhanced by inhibition of CD36 palmitoylation, either by mutations of palmitoylation sites (AA-SS) of CD36 or pharmacological agents 2BP in HepG2 cells. This could be due to a reduction of

the amount of CD36/Fyn complex on the hepatic plasma membrane. Therefore, our results suggest that increased palmitoylation of CD36 may impair FA  $\beta$ -oxidation and that inhibition of CD36 palmitoylation may activate AMPK in a Fyn-LKB1 manner, improving FA  $\beta$ -oxidation and preventing steatosis.

On the basis of our findings, we postulate that enhanced CD36 palmitoylation, which occurred in the presence of a high-fat diet, promotes CD36 translocation to the plasma membrane of hepatocytes, facilitating LCFA binding/uptake and CD36/Fyn/Lyn complex formation. The imbalance between FA uptake and consumption (FAO), as well as activation of the inflammatory response, contributes to the development of NASH. Prevention of palmitoylation hinders CD36 in the cytoplasm, which reduces lipid uptake, inhibits inflammatory responses by inhibition of JNK signaling pathway and improves FA  $\beta$ -oxidation by activation of AMPK signaling pathway with an overall amelioration of NASH (Figure 8).

In conclusion, the present study provides sound evidence for suggesting that distribution of CD36 on cellular plasma membrane, rather than simply its level of expression, plays a key role in the pathogenesis of NASH. As palmitoylation controls the distribution and functions of CD36, targeting the palmitoylation sites of CD36 may offer a new therapeutic strategy for the treatment of NASH and its progression to advanced chronic liver disease.

## References

- [1] Lazo M, Hernaez R, Eberhardt MS, Bonekamp S, Kamel I, Guallar E, et al. Prevalence of nonalcoholic fatty liver disease in the United States: the Third National Health and Nutrition Examination Survey, 1988-1994. *Am J Epidemiol* 2013;178:38-45.
- [2] Wong VW. Nonalcoholic fatty liver disease in Asia: a story of growth. *J Gastroenterol Hepatol* 2013;28:18-23.
- [3] Flegal KM, Carroll MD, Kit BK, Ogden CL. Prevalence of obesity and trends in the distribution of body mass index among US adults, 1999-2010. *JAMA* 2012;307:491-497.
- [4] Yoshimura K, Okanoue T, Ebise H, Iwasaki T, Mizuno M, Shima T, et al. Identification of novel noninvasive markers for diagnosing nonalcoholic steatohepatitis and related fibrosis by data mining. *Hepatology* 2016;63:462-473.
- [5] Marengo A, Jouness RI, Bugianesi E. Progression and Natural History of Nonalcoholic Fatty Liver Disease in Adults. *Clin Liver Dis* 2016;20:313-324.
- [6] Wong VW, Wong GL, Chim AM, Tse AM, Tsang SW, Hui AY, et al. Validation of the NAFLD fibrosis score in a Chinese population with low prevalence of advanced fibrosis. *Am J Gastroenterol* 2008;103:1682-1688.
- [7] Sayiner M, Koenig A, Henry L, Younossi ZM. Epidemiology of Nonalcoholic Fatty Liver Disease and Nonalcoholic Steatohepatitis in the United States and the Rest of the World. *Clin Liver Dis* 2016;20:205-214.
- [8] Hames KC, Vella A, Kemp BJ, Jensen MD. Free fatty acid uptake in humans with CD36 deficiency. *Diabetes* 2014;63:3606-3614.
- [9] Coburn CT, Knapp FF, Jr., Febbraio M, Beets AL, Silverstein RL, Abumrad NA. Defective uptake and utilization of long chain fatty acids in muscle and adipose tissues of CD36 knockout mice. *J Biol Chem* 2000;275:32523-32529.
- [10] Samovski D, Sun J, Pietka T, Gross RW, Eckel RH, Su X, et al. Regulation of AMPK activation by CD36 links fatty acid uptake to beta-oxidation. *Diabetes* 2015;64:353-359.
- [11] Stewart CR, Stuart LM, Wilkinson K, van Gils JM, Deng J, Halle A, et al. CD36 ligands promote sterile inflammation through assembly of a Toll-like receptor 4 and 6 heterodimer. *Nat Immunol* 2010;11:155-161.
- [12] Sheedy FJ, Grebe A, Rayner KJ, Kalantari P, Ramkhelawon B, Carpenter SB, et al.

CD36 coordinates NLRP3 inflammasome activation by facilitating intracellular nucleation of soluble ligands into particulate ligands in sterile inflammation. *Nat Immunol* 2013;14:812-820.

[13] Kennedy DJ, Kuchibhotla S, Westfall KM, Silverstein RL, Morton RE, Febbraio M. A CD36-dependent pathway enhances macrophage and adipose tissue inflammation and impairs insulin signalling. *Cardiovasc Res* 2011;89:604-613.

[14] Abumrad NA, Goldberg IJ. CD36 actions in the heart: Lipids, calcium, inflammation, repair and more? *Biochim Biophys Acta* 2016;1861:1442-1449.

[15] Greco D, Kotronen A, Westerbacka J, Puig O, Arkkila P, Kiviluoto T, et al. Gene expression in human NAFLD. *Am J Physiol Gastrointest Liver Physiol* 2008;294:G1281-1287.

[16] Garcia-Monzon C, Lo Iacono O, Crespo J, Romero-Gomez M, Garcia-Samaniego J, Fernandez-Bermejo M, et al. Increased soluble CD36 is linked to advanced steatosis in nonalcoholic fatty liver disease. *Eur J Clin Invest* 2014;44:65-73.

[17] Koonen DP, Jacobs RL, Febbraio M, Young ME, Soltys CL, Ong H, et al. Increased hepatic CD36 expression contributes to dyslipidemia associated with diet-induced obesity. *Diabetes* 2007;56:2863-2871.

[18] Wilson CG, Tran JL, Erion DM, Vera NB, Febbraio M, Weiss EJ. Hepatocyte-Specific Disruption of CD36 Attenuates Fatty Liver and Improves Insulin Sensitivity in HFD-Fed Mice. *Endocrinology* 2016;157:570-585.

[19] Pohl J, Ring A, Eehalt R, Schulze-Bergkamen H, Schad A, Verkade P, et al. Long-chain fatty acid uptake into adipocytes depends on lipid raft function. *Biochemistry* 2004;43:4179-4187.

[20] Wallin T, Ma Z, Ogata H, Jorgensen IH, Iezzi M, Wang H, et al. Facilitation of fatty acid uptake by CD36 in insulin-producing cells reduces fatty-acid-induced insulin secretion and glucose regulation of fatty acid oxidation. *Biochim Biophys Acta* 2010;1801:191-197.

[21] Rocks O, Gerauer M, Vartak N, Koch S, Huang ZP, Pechlivanis M, et al. The palmitoylation machinery is a spatially organizing system for peripheral membrane proteins. *Cell* 2010;141:458-471.

[22] Tao N, Wagner SJ, Lublin DM. CD36 is palmitoylated on both N- and C-terminal

cytoplasmic tails. *J Biol Chem* 1996;271:22315-22320.

[23] Thorne RF, Ralston KJ, de Bock CE, Mhaidat NM, Zhang XD, Boyd AW, et al. Palmitoylation of CD36/FAT regulates the rate of its post-transcriptional processing in the endoplasmic reticulum. *Biochim Biophys Acta* 2010;1803:1298-1307.

[24] Brigidi GS, Bamji SX. Detection of protein palmitoylation in cultured hippocampal neurons by immunoprecipitation and acyl-biotin exchange (ABE). *J Vis Exp* 2013; 18: pii: 50031.

[25] Thorne RF, Marshall JF, Shafren DR, Gibson PG, Hart IR, Burns GF. The integrins alpha3beta1 and alpha6beta1 physically and functionally associate with CD36 in human melanoma cells. Requirement for the extracellular domain OF CD36. *J Biol Chem* 2000;275:35264-35275.

[26] Tzircotis G, Thorne RF, Isacke CM. A new spreadsheet method for the analysis of bivariate flow cytometric data. *BMC Cell Biol* 2004;5:10.

[27] Chavda B, Arnott JA, Planey SL. Targeting protein palmitoylation: selective inhibitors and implications in disease. *Expert Opin Drug Discov* 2014:1-15.

[28] Pohl J, Ring A, Korkmaz U, Eehalt R, Stremmel W. FAT/CD36-mediated long-chain fatty acid uptake in adipocytes requires plasma membrane rafts. *Mol Biol Cell* 2005;16:24-31.

[29] Raney MA, Turcotte LP. Evidence for the involvement of CaMKII and AMPK in Ca<sup>2+</sup>-dependent signaling pathways regulating FA uptake and oxidation in contracting rodent muscle. *J Appl Physiol* (1985) 2008;104:1366-1373.

[30] Kodama Y, Kisseleva T, Iwaisako K, Miura K, Taura K, De Minicis S, et al. c-Jun N-terminal kinase-1 from hematopoietic cells mediates progression from hepatic steatosis to steatohepatitis and fibrosis in mice. *Gastroenterology* 2009;137:1467-1477 e1465.

[31] Glatz JF, Luiken JJ. From fat to FAT (CD36/SR-B2): Understanding the regulation of cellular fatty acid uptake. *Biochimie* 2017;136:21-26.

[32] Miquilena-Colina ME, Lima-Cabello E, Sanchez-Campos S, Garcia-Mediavilla MV, Fernandez-Bermejo M, Lozano-Rodriguez T, et al. Hepatic fatty acid translocase CD36 upregulation is associated with insulin resistance, hyperinsulinaemia and increased steatosis in non-alcoholic steatohepatitis and chronic hepatitis C. *Gut* 2011;60:1394-1402.

- [33] Yang X, Okamura DM, Lu X, Chen Y, Moorhead J, Varghese Z, et al. CD36 in chronic kidney disease: novel insights and therapeutic opportunities. *Nat Rev Nephrol* 2017;13:769-781.
- [34] Jochen A, Hays J. Purification of the major substrate for palmitoylation in rat adipocytes: N-terminal homology with CD36 and evidence for cell surface acylation. *J Lipid Res* 1993;34:1783-1792.
- [35] van Oort MM, Drost R, Janbetaen L, Van Doorn JM, Kerver J, Van der Horst DJ, et al. Each of the four intracellular cysteines of CD36 is essential for insulin- or AMP-activated protein kinase-induced CD36 translocation. *Arch Physiol Biochem* 2014;120:40-49.
- [36] Eyre NS, Cleland LG, Tandon NN, Mayrhofer G. Importance of the carboxyl terminus of FAT/CD36 for plasma membrane localization and function in long-chain fatty acid uptake. *J Lipid Res* 2007;48:528-542.
- [37] Tuncman G, Hirosumi J, Solinas G, Chang L, Karin M, Hotamisligil GS. Functional in vivo interactions between JNK1 and JNK2 isoforms in obesity and insulin resistance. *Proc Natl Acad Sci U S A* 2006;103:10741-10746.
- [38] Schattenberg JM, Singh R, Wang Y, Lefkowitz JH, Rigoli RM, Scherer PE, et al. JNK1 but not JNK2 promotes the development of steatohepatitis in mice. *Hepatology* 2006;43:163-172.
- [39] Chen K, Febbraio M, Li W, Silverstein RL. A specific CD36-dependent signaling pathway is required for platelet activation by oxidized low-density lipoprotein. *Circ Res* 2008;102:1512-1519.
- [40] Zhao L, Zhong S, Qu H, Xie Y, Cao Z, Li Q, et al. Chronic inflammation aggravates metabolic disorders of hepatic fatty acids in high-fat diet-induced obese mice. *Scientific Reports* 2015;5:10222.
- [41] Guo Y, Walther TC, Rao M, Stuurman N, Goshima G, Terayama K, et al. Functional genomic screen reveals genes involved in lipid-droplet formation and utilization. *Nature* 2008;453:657-661.
- [42] Day EA, Ford RJ, Steinberg GR. AMPK as a Therapeutic Target for Treating Metabolic Diseases. *Trends Endocrinol Metab* 2017;28:545-560.
- [43] Woods A, Williams JR, Muckett PJ, Mayer FV, Liljevald M, Bohlooly YM, et al.

Liver-Specific Activation of AMPK Prevents Steatosis on a High-Fructose Diet. *Cell Rep* 2017;18:3043-3051.

[44] Zeng J, Deng S, Wang Y, Li P, Tang L, Pang Y. Specific Inhibition of Acyl-CoA Oxidase-1 by an Acetylenic Acid Improves Hepatic Lipid and Reactive Oxygen Species (ROS) Metabolism in Rats Fed a High Fat Diet. *J Biol Chem* 2017;292:3800-3809.

[45] Yamada E, Pessin JE, Kurland IJ, Schwartz GJ, Bastie CC. Fyn-dependent regulation of energy expenditure and body weight is mediated by tyrosine phosphorylation of LKB1. *Cell Metab* 2010;11:113-124.

ACCEPTED MANUSCRIPT

### Figure legends

**Fig.1. CD36 localization at hepatocytes plasma membrane was significantly increased in the liver of patients with NASH.** Human liver tissue samples were obtained from patients undergoing liver biopsy for diagnostic purposes. Subjects were subdivided into those with normal liver (NL, n=20), simple steatosis (SS, n=19), non-alcoholic steatohepatitis (NASH, n=21) and cirrhosis (n=19). (A) Representative pictures of HE staining of human livers. (B) Hepatic steatosis index. (C) Sirius red staining. (D) Hepatic fibrosis index. (E) Dual-immunofluorescent staining of CD36 and  $\beta$ -catenin on sections from human livers. (F) Pearson's correlation (R value) of CD36 and  $\beta$ -catenin. (G) Colocalization rate of CD36 and  $\beta$ -catenin. Data are presented as mean  $\pm$  SEM. The differences among four groups were statistically analyzed by one-way ANOVA with Tukey's multiple comparisons test. \* P<0.05 vs. CTL, # P<0.05 vs. SS, \$ P<0.05 vs. NASH.

**Fig.2. CD36 palmitoylation was induced in the liver of mice with NASH.** The C57BL/6J mice were fed with a normal chow diet (NCD) or high fat diet (HFD) for 22 weeks (n=6). (A) Histopathological examination of C57BL/6J livers. Representative pictures of HE staining (i, ii), ORO staining (iii, iv) and Sirius red staining (v, vi) in liver sections from mice with NCD and HFD were shown. (B) Hepatic steatosis index and hepatic fibrosis index. (C) Protein levels of TNF $\alpha$  in mice livers (n=4). (D) Protein levels of CD36 in mice livers (n=4). (E) Dual-immunofluorescent staining of CD36 and  $\beta$ -catenin on sections from mice livers (n=6). (F) Pearson's correlation (R value) and co-localization rate of CD36 and  $\beta$ -catenin. (G) Protein levels of palmitoylated CD36 in mice livers (n=3). Data were presented as mean  $\pm$  SEM. The difference between two groups was statistically analyzed by Student's t-test. \* P<0.05 vs. NCD.

**Fig.3. Inhibition of CD36 palmitoylation protected mice from NASH.** Lentivirus vectors expressing negative control (NC), wildtype CD36 (wt-CD36) and palmitoylation sites-mutated CD36 (AA-SS CD36) were injected into CD36

knockout (CD36KO) mice via tail vein. (A) Dual-immunofluorescent staining of CD36 and  $\beta$ -catenin on mice livers (n=6). (B) Pearson's correlation (R value) of CD36 and  $\beta$ -catenin. (C) Colocalization rate of CD36 and  $\beta$ -catenin. (D) Representative pictures of HE staining (i, ii, iii), ORO staining (iv, v, vi) and Sirius red staining (vii, viii, ix) in mice liver sections were shown. (E) Hepatic contents of triglycerides (TG) (n=6). (F) Relative mRNA levels of MCP-1, TNF $\alpha$ , IL-6. (G) Relative mRNA levels of collIV and TGF $\beta$  in mice livers (n=6). Data were presented as mean  $\pm$  SEM. The differences among three groups were statistically analyzed by one-way ANOVA with Tukey's multiple comparisons test. \* P<0.05 vs. NC groups, # P<0.05 vs. wt-CD36 groups.

**Fig.4. Inhibition of CD36 palmitoylation influences protein hydrophobicity and its localization at hepatocytes plasma membrane.**

(A) The hydrophobicity values of wt-CD36 (blue) and AA-SS CD36 protein (red). (B) The Grand Average of Hydrophobicity (GRAVY) of wt-CD36 and AA-SS CD36 protein. (C) The accessible surface area of wt-CD36 and AA-SS CD36 protein. Lentivirus expressing NC-vector, wt-CD36, AA-SS CD36 were incubated with HepG2 cells and stable cell lines were selected with puromycin. Before harvest, cells were incubated with serum-free medium for 12h, followed by 24h of palmitate (PA) treatments. (D) Total CD36 expression was detected using FACS. (E). The cytosol and plasma membrane fraction were isolated from cells and CD36 expression in these fractions were analyzed by western blot. The ratio of CD36 expression in plasma membrane to cytoplasm was significantly lower in AA-SS HepG2 cells than in wt-CD36 HepG2 cells (mean  $\pm$  SEM; n = 3). (F) Detergent-resistant membrane (DRM) and non-DRM were isolated and analyzed for CD36 expression. Inhibition of palmitoylation reduced the localization of CD36 in lipid raft (mean  $\pm$  SEM; n = 3). Data were presented as mean  $\pm$  SEM. The difference between two groups was statistically analyzed by Student's t-test. The differences among three groups were statistically analyzed by one-way ANOVA with Tukey's multiple comparisons test. \* P<0.05 vs. NC groups, # P<0.05 vs. wt-CD36 groups.

**Fig.5. Inhibition of CD36 palmitoylation reduces long-chain fatty acid (LCFA) binding/uptake and CD36/Fyn/Lyn complex formation in hepG2 cells.** The wt-CD36 and AA-SS CD36 HepG2 cells were incubated with serum-free medium for 12h, followed by 24h of 0.16mM palmitate (PA) treatments. HepG2 cells were treated with PA or PA plus 2BP for 24h. Then cells were incubated with FL-C16 for 1h at 4°C (A) and 37°C (B) and labeled with PE-CD36, followed by a bivariate FACS analysis. (A) Low-capability of LCFA binding in AA-SS HepG2 cells. (B) Low-capability of LCFA uptake in AA-SS HepG2 cells. (C) 2BP reduced the capability of HepG2 cells binding LCFA. (D) 2BP reduced the uptake of LCFA in HepG2 cells. (E) Co-immunoprecipitations of CD36 and Fyn/Lyn in cells (n=3). Data were presented as mean  $\pm$  SEM. The difference between two groups was statistically analyzed by Student's t-test. \* P<0.05 vs.wt-CD36 groups.

**Fig.6. Inhibition of CD36 palmitoylation enhances FA  $\beta$ -oxidation via activating AMPK pathway.** Cells were incubated with substrate-limited medium for 12h, followed by FA oxidation (FAO) analysis using seahorse system. (A) Palmitate-dependent OCR in NC HepG2 and wt-CD36 HepG2 cells (n=8). (B) Palmitate-dependent OCR in wt-CD36 and AA-SS CD36 HepG2 cells (n=8). (C) palmitate-dependent OCR in 2BP-treated HepG2 cells (n = 8). (D-I) NC, wt-CD36 and AA-SS CD36 HepG2 cells were incubated with substrate-limited medium for 12h, followed by 2h of 0.16mM palmitate (PA) treatments. HepG2 cells were treated with PA or PA plus 2BP for 24h. (D) Western blot of phosphorylated AMPK and AMPK in NC, wt-CD36 and AA-SS HepG2 cells (n=3). Data were presented as mean  $\pm$  SEM. \* P<0.05 vs. NC groups, # P<0.05 vs. wt-CD36 groups. (E) Protein levels of phosphorylated AMPK and AMPK in 2-BP treated HepG2 cells (n=3). \* P<0.05 vs. PA. (F-I) Cells were pretreated with 10mM Compound C (CC). (F) Basal and maximal FAO in AA-SS HepG2 treated with compound C. \* P<0.05 AA-SS groups without compound C treatment. (G) Bodipy staining for lipid droplets in NC, wt-CD36, AA-SS-HepG2 cells and in control (ctl, 0mM PA),

palmitate (0.16mM PA) and palmitate plus 2BP (0.16mM PA+2BP) treated cells (H) in absence and presence of compound C. (I) Quantitative data of lipid droplets in HepG2 cells. Data were presented as mean  $\pm$  SEM. The difference between two groups was statistically analyzed by Student's t-test. The differences among three or more groups were statistically analyzed by one-way ANOVA with Tukey's multiple comparisons test. \*  $P < 0.05$  vs.ctl, #  $P < 0.05$  vs.PA, \$  $P < 0.05$  vs. cells without compound C treatment.

**Fig.7. Inhibition of palmitoylation reduces inflammation via inhibiting JNK pathway.** NC-HepG2, wt-CD36-HepG2 and AA-SS-HepG2 cells were incubated with serum-free medium for 12h, followed by 24h of palmitate treatments. (A) NF- $\kappa$ B activities in NC, wt-CD36 and AA-SS HepG2 cells (n=8). (B) Protein levels of TNF $\alpha$  in NC, wt-CD36 and AA-SS HepG2 cells (n=3) and in 2-BP treated HepG2 cells (C, n=3). (D) NC-HepG2 and wt-CD36-HepG2 were treated with sp600125 (sp, 10mM), the mRNA levels of TNF $\alpha$  were measured by RT-PCR (n=6). (E) Protein levels of JNK and phosphorylated JNK in NC, wt-CD36 and AA-SS HepG2 cells (n=3) and in 2-BP treated HepG2 cells (F, n=3). Data were presented as mean  $\pm$  SEM. The difference between two groups was statistically analyzed by Student's t-test. The differences among three groups were statistically analyzed by one-way ANOVA with Tukey's multiple comparisons test. \*  $P < 0.05$  vs. NC groups or PA, #  $P < 0.05$  vs. wt-CD36 groups.

**Fig.8. Molecular mechanisms by which inhibition CD36 palmitoylation protects mice from NASH.** High-fat diet enhances CD36 palmitoylation, promoting CD36 locations in plasma membrane, facilitating LCFA binding/uptake and CD36/Fyn/Lyn complex formation. The imbalance between FA availability (uptake) and consumption (FAO), as well as activation of inflammatory response, results in the development of NASH. When CD36 palmitoylation was inhibited, JNK-mediated inflammatory signaling transduction is inhibited and cellular FA homeostasis is recovered, protecting the pathogenesis of NASH.

Supplementary Fig.1. (A) HepG2 cells were treated with different concentrations of palmitate (0, 0.04, 0.16, 0.64mM of PA) for 24h. PA dose-dependently increased CD36 mRNA expression in HepG2 cells (n=8). (B) HepG2 cells were treated with 0.16mM PA for 24h. The palmitoylated CD36 levels in HepG2 cells were detected using IP-ABE method (n=3). (C) The contents of free fatty acid (FFA) in serum were increased in C57BL/6J mice with HFD-feeding compared with mice with NCD (n=6). Data were presented as mean  $\pm$  SEM. \* P<0.05 vs. 0mM PA (Control) or NCD, # P<0.05 vs.0.04mM PA, \$ P<0.05 vs.0.16mM PA.

Supplementary Fig.2. (A) Schematic of the mutation on palmitoylation sites of wide-type CD36. Lentivirus expressing NC-vector, wt-CD36, AA-SS CD36 were incubated with HepG2 cells and stable cell lines were selected with puromycin. (B) High-level of CD36 expression in wt-CD36-HepG2 and AA-SS -HepG2 cells. (C) The palmitoylated CD36 were increased in wt-CD36-HepG2 cells, not in AA-SS-HepG2. (D) Lentivirus expressing NC-vector, wt-CD36, AA-SS CD36 were injected into CD36 knockout mice via tail vein, followed by a 8-week high fat diet treatment. CD36 expression in mice livers was detected by western blot (n=4).

Supplementary Fig.3. The predicted N-terminal and C-terminal protein structures of palmitoylated CD36 and non-palmitoylated CD36.

Fig. 1.

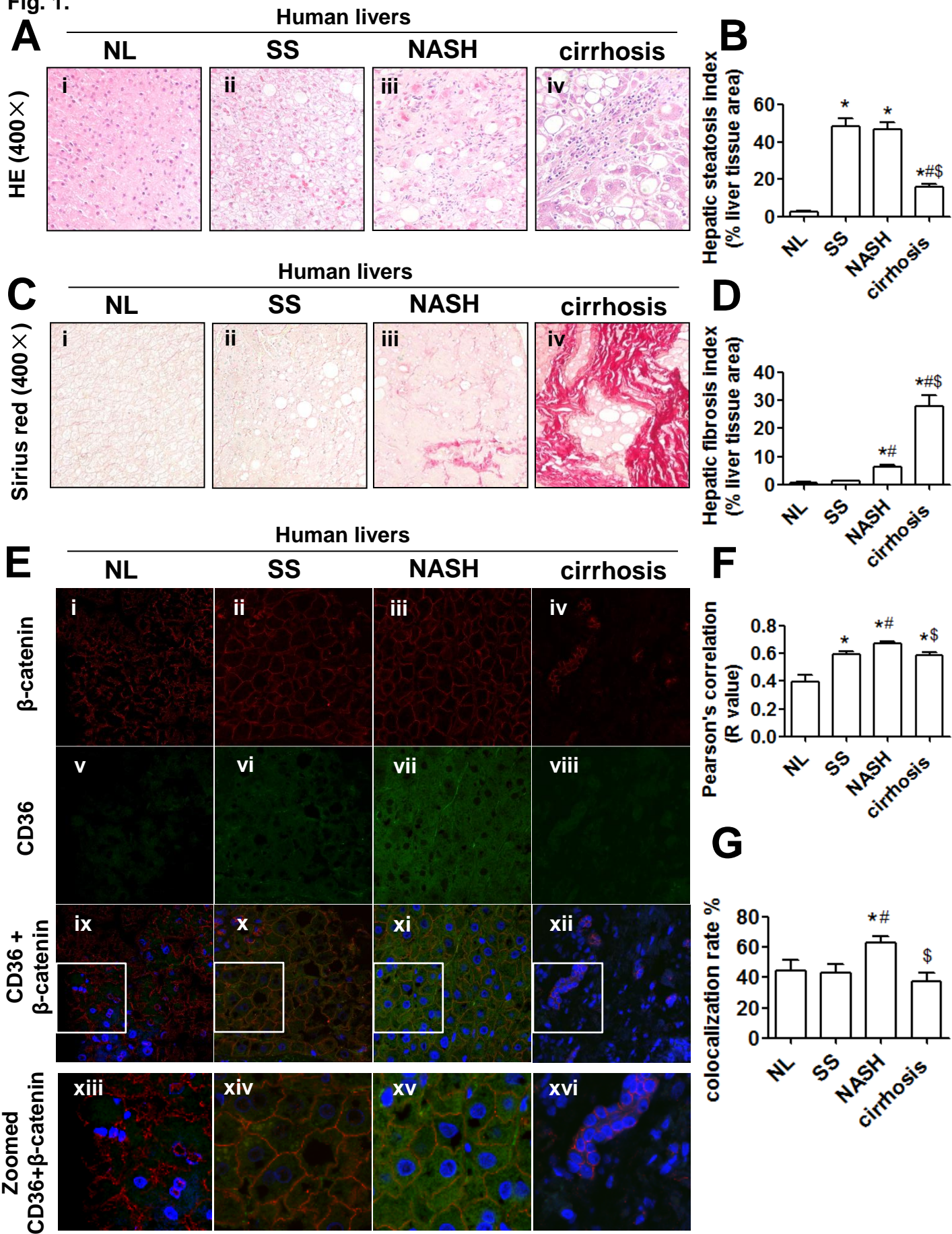


Fig. 2.

C57 Mice livers

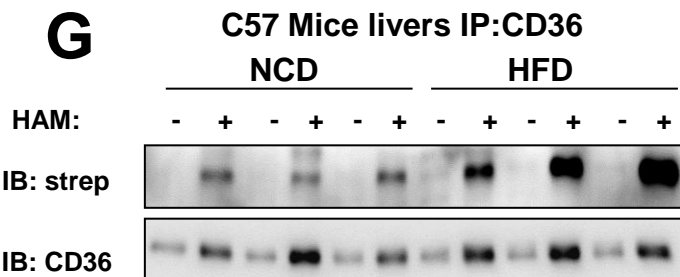
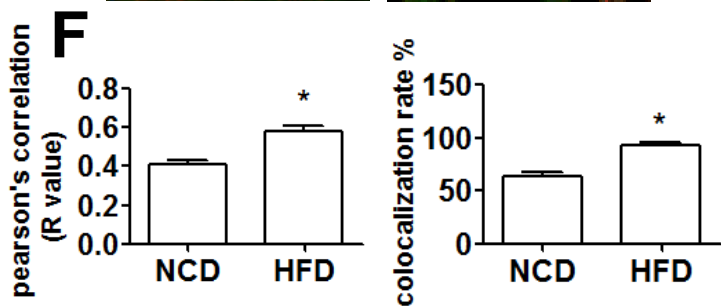
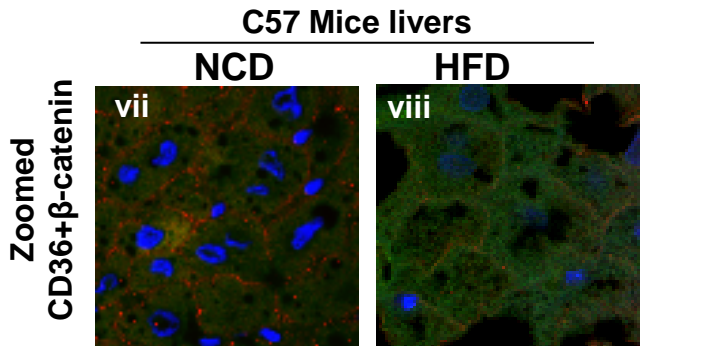
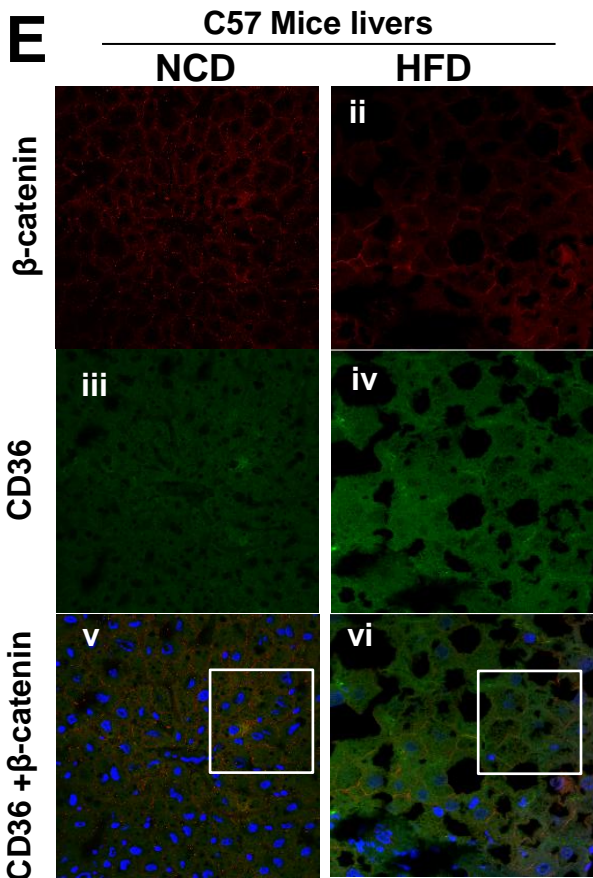
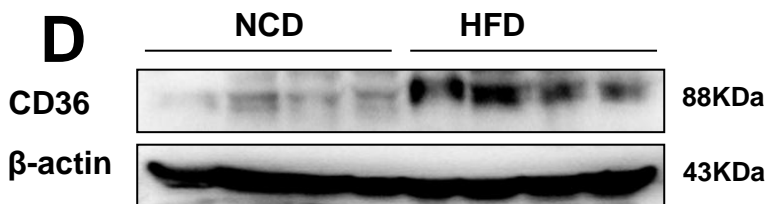
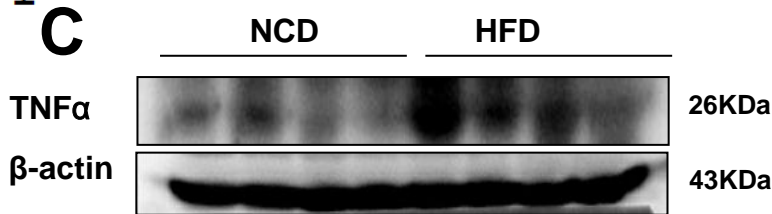
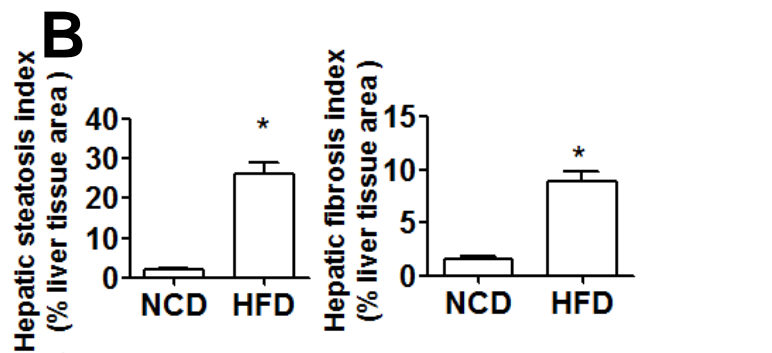
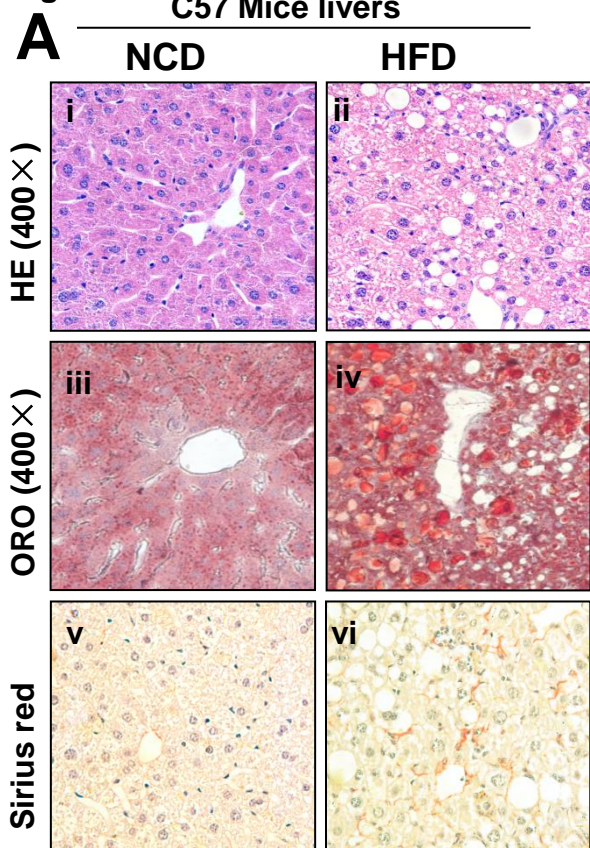


Fig. 3.

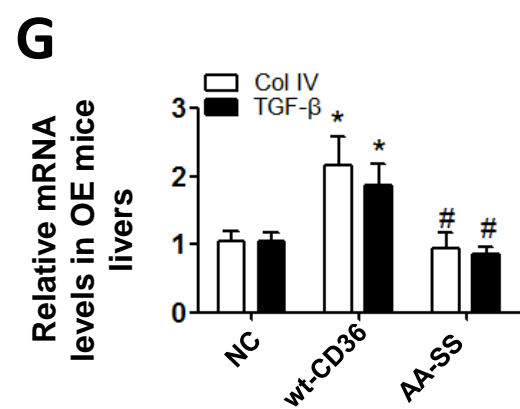
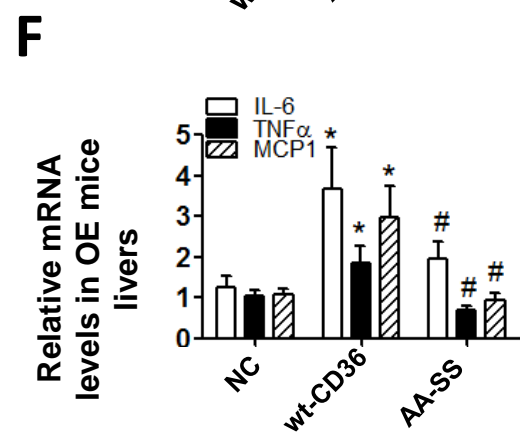
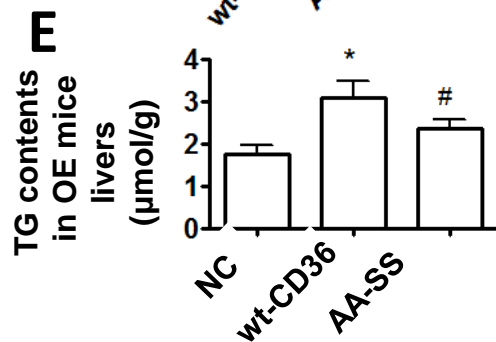
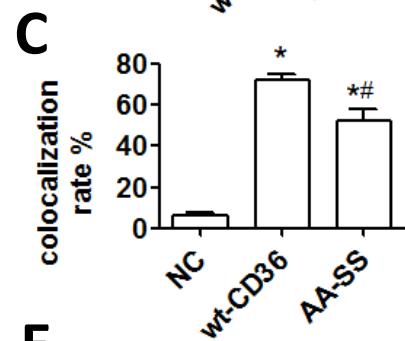
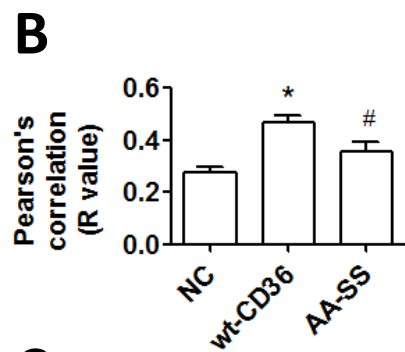
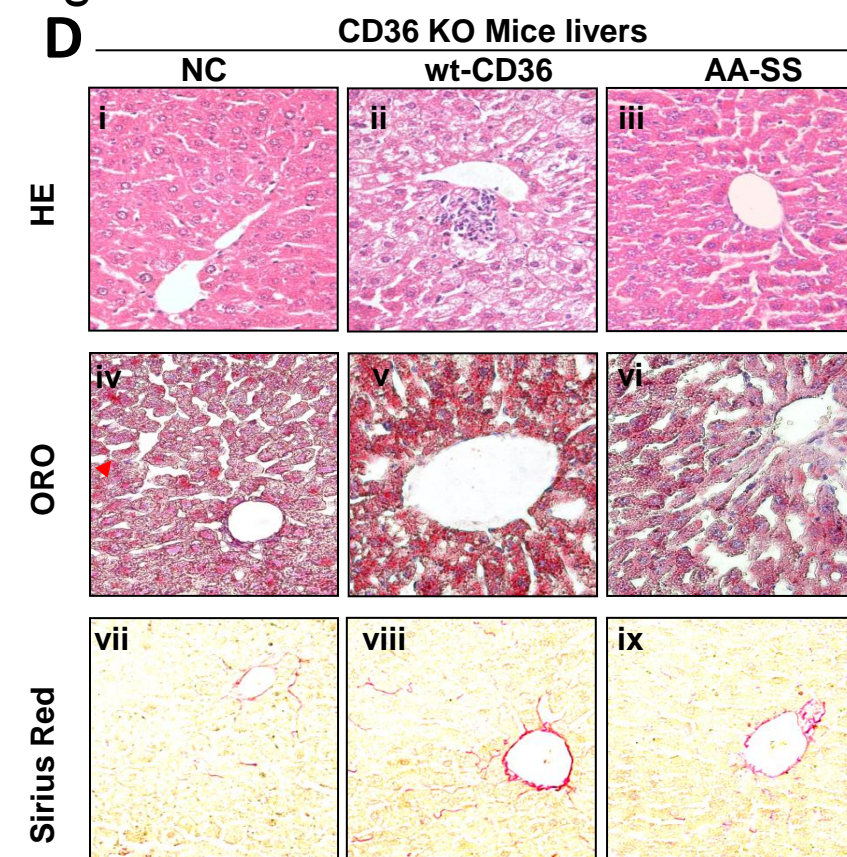
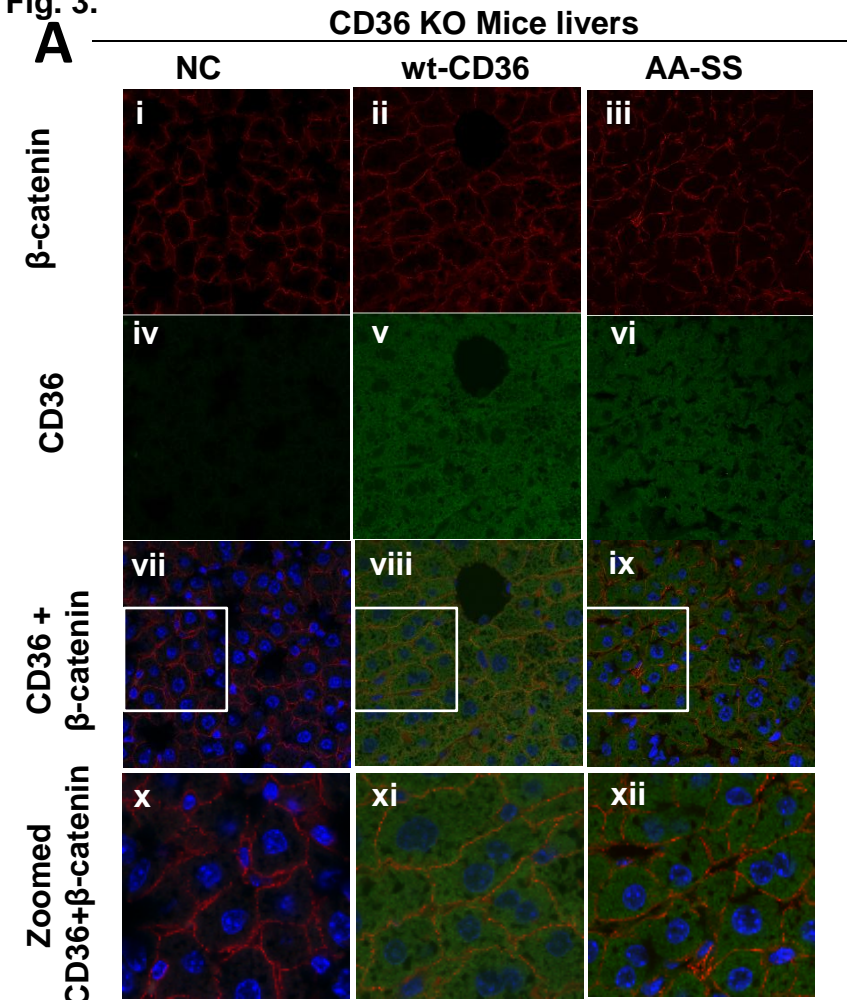
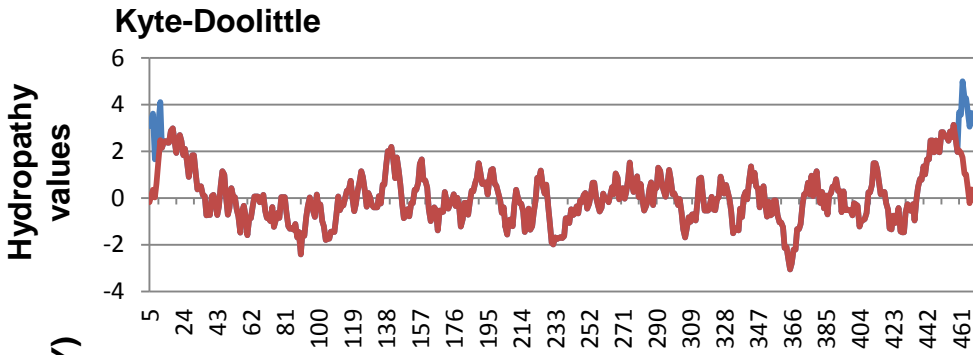
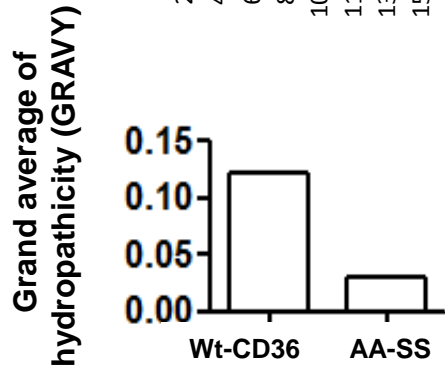


Fig. 4.

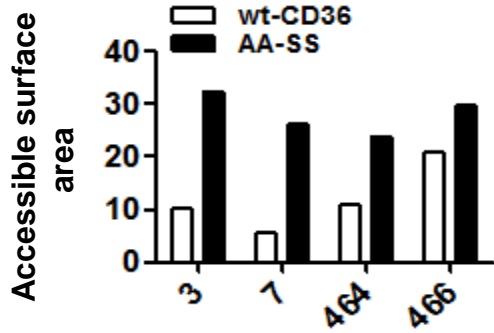
**A**



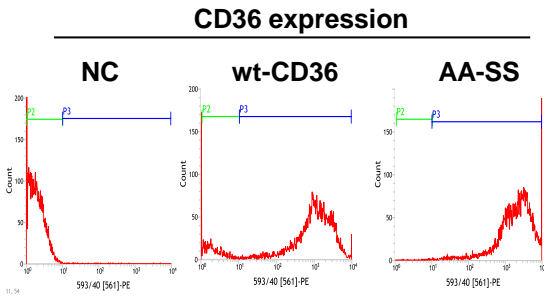
**B**



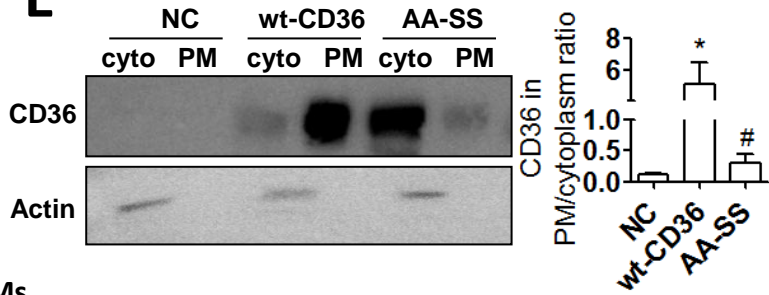
**C**



**D**



**E**



**F**

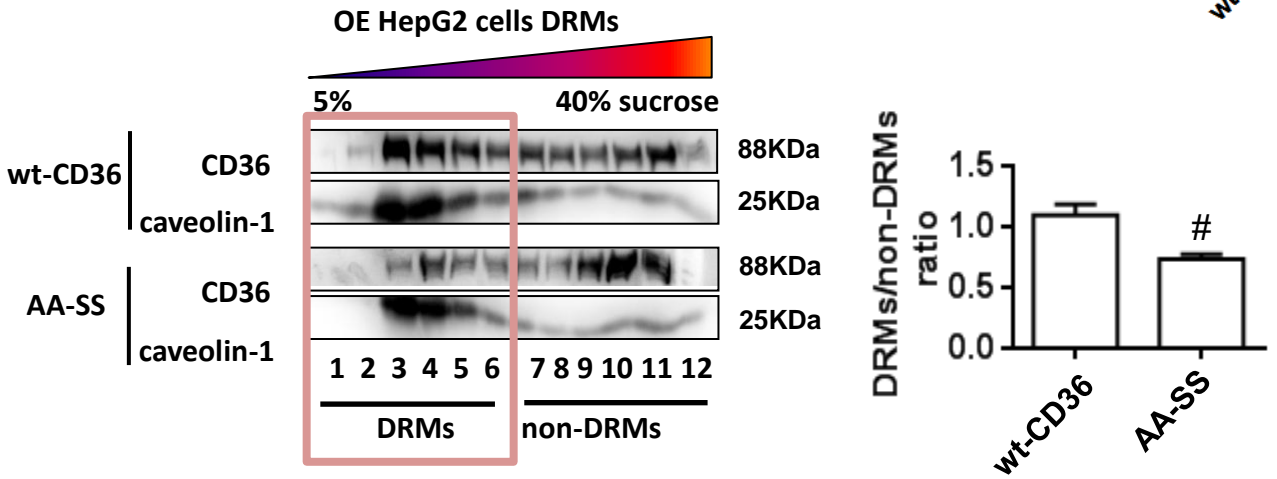
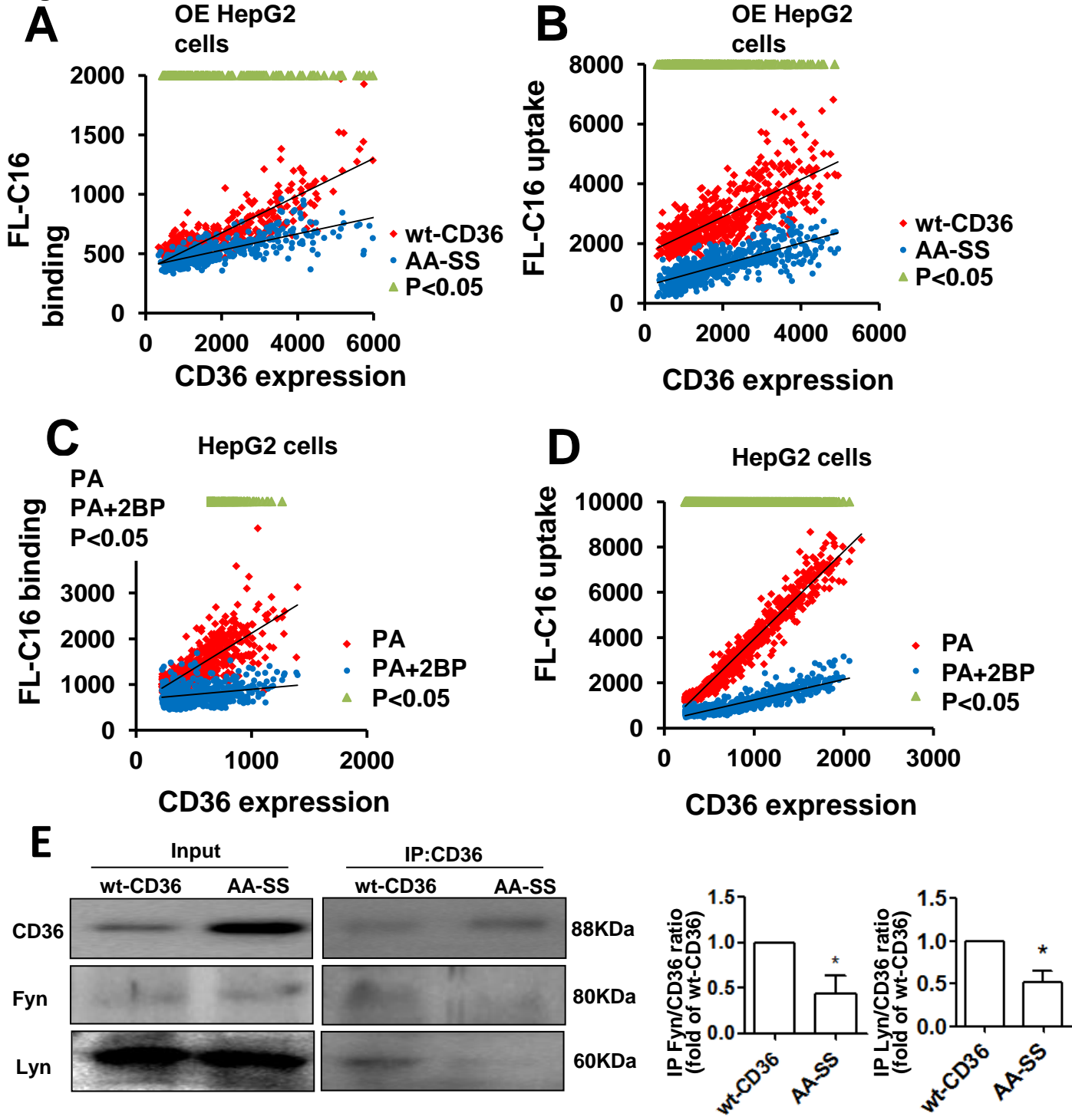


Fig. 5.



**Fig. 6.**

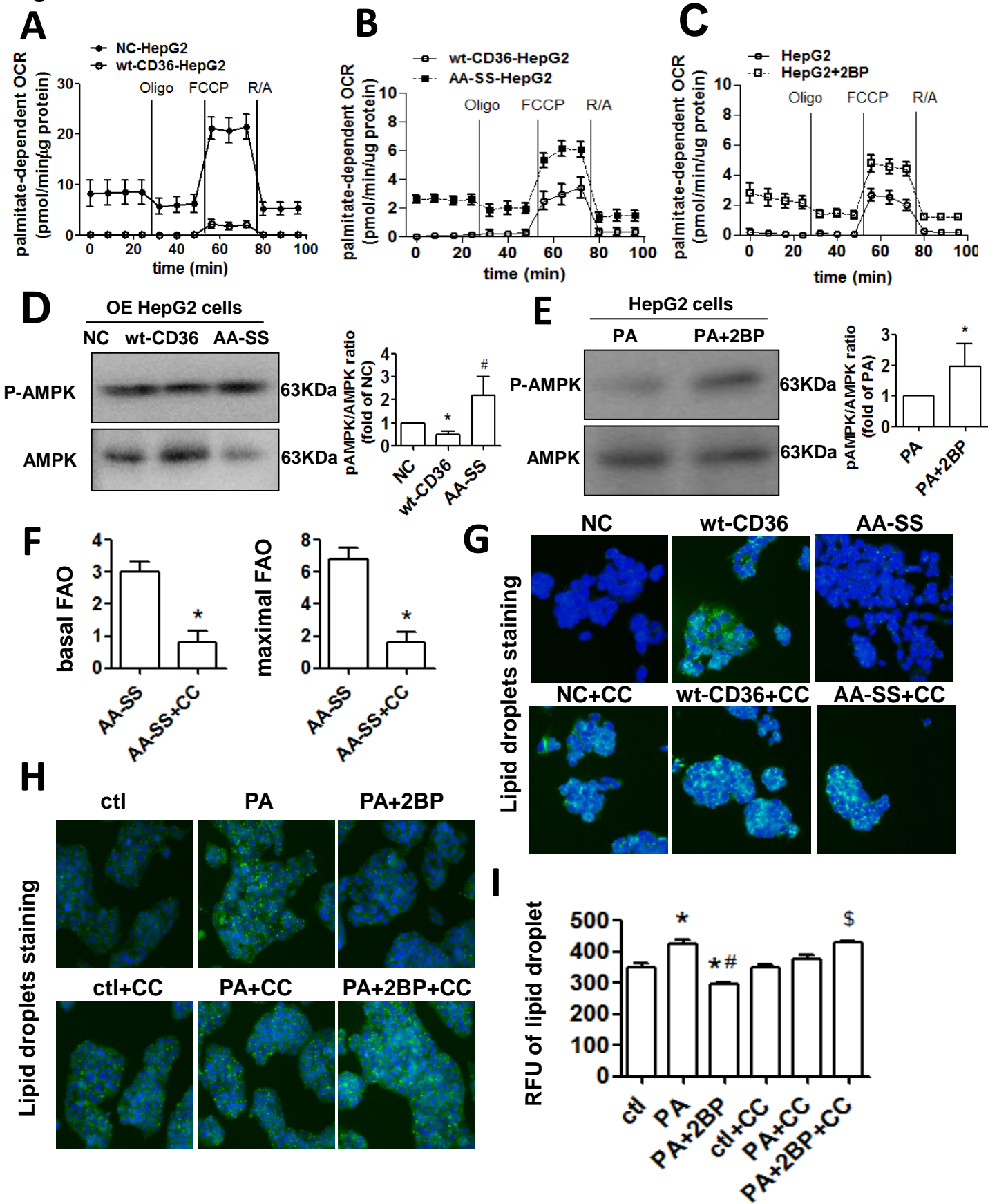


Fig. 7.

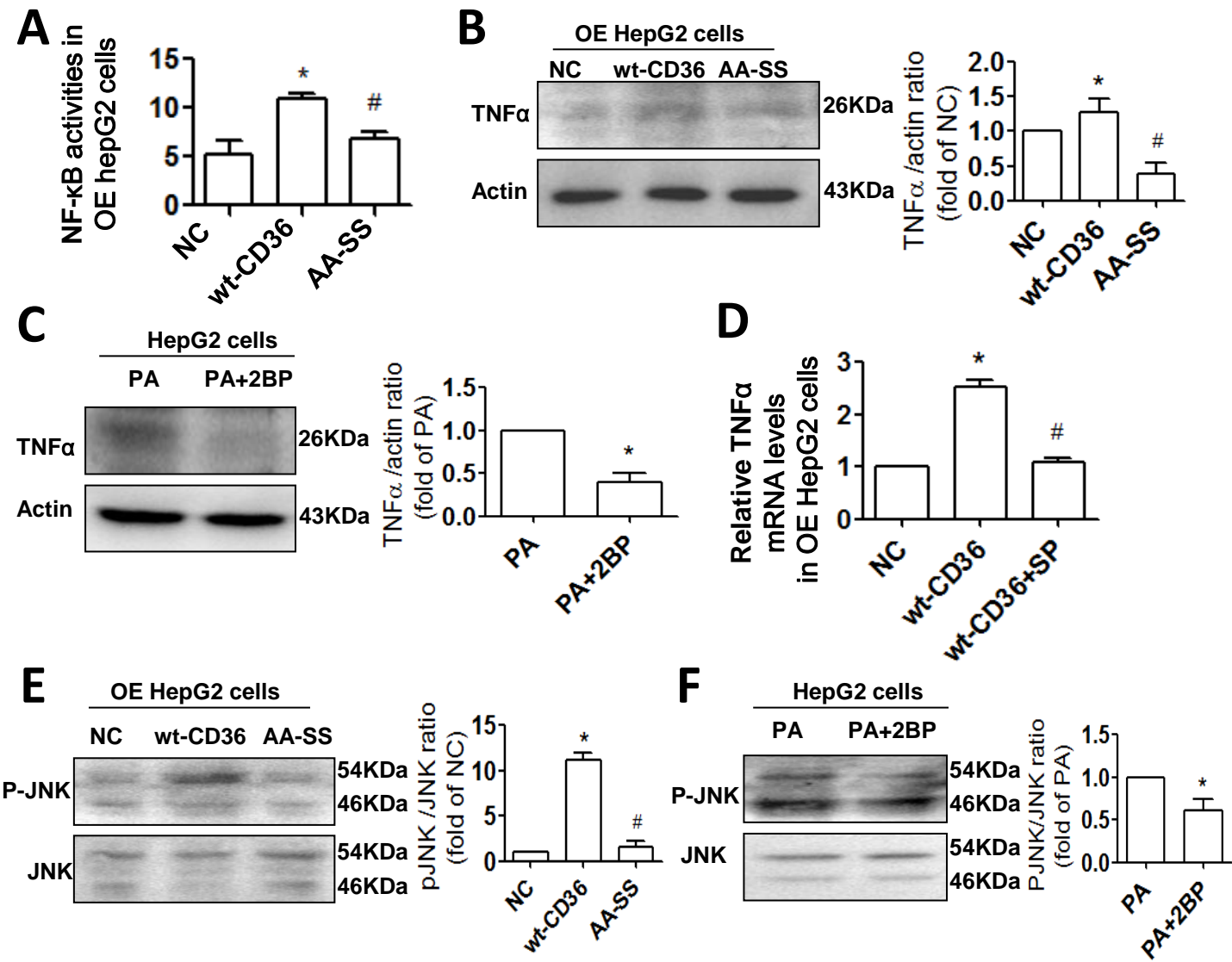
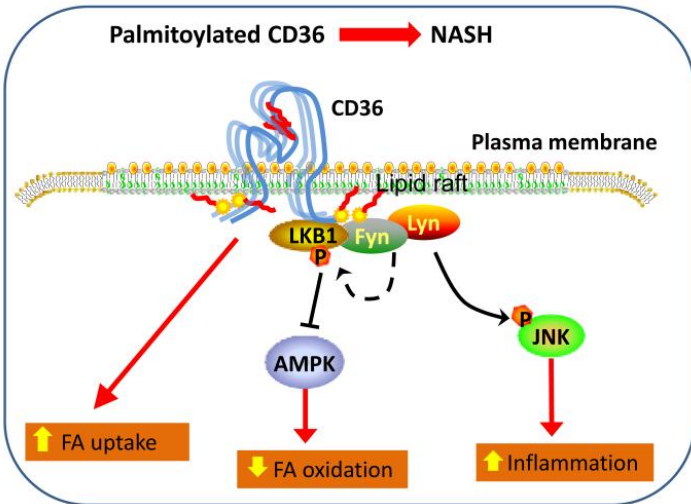
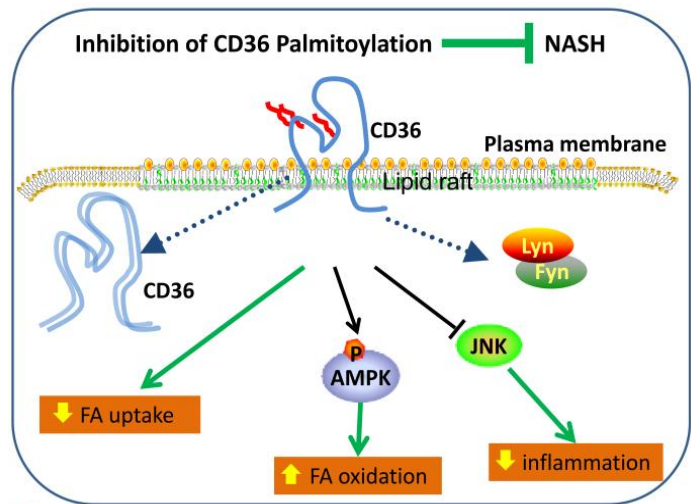


Fig. 8.

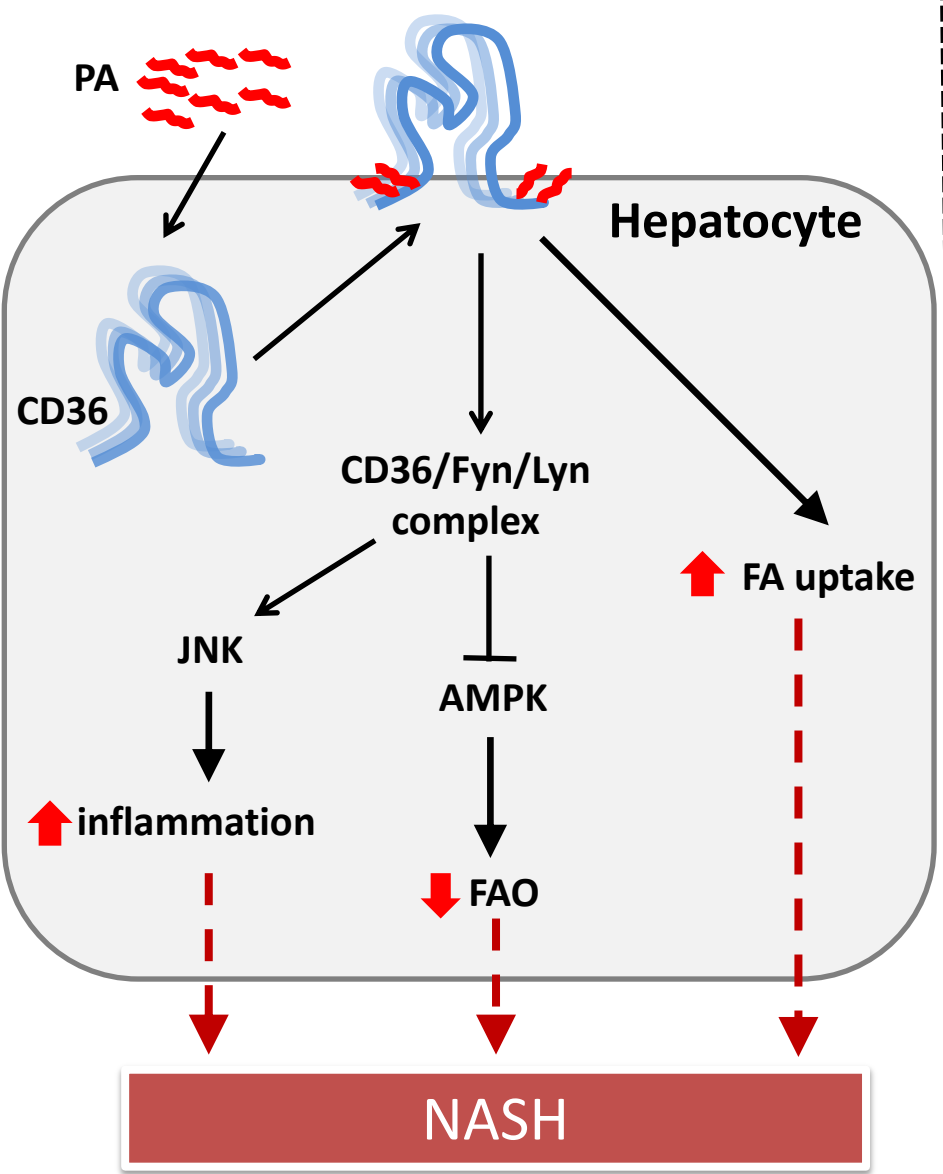


● cystein  
~ Palmitic acid

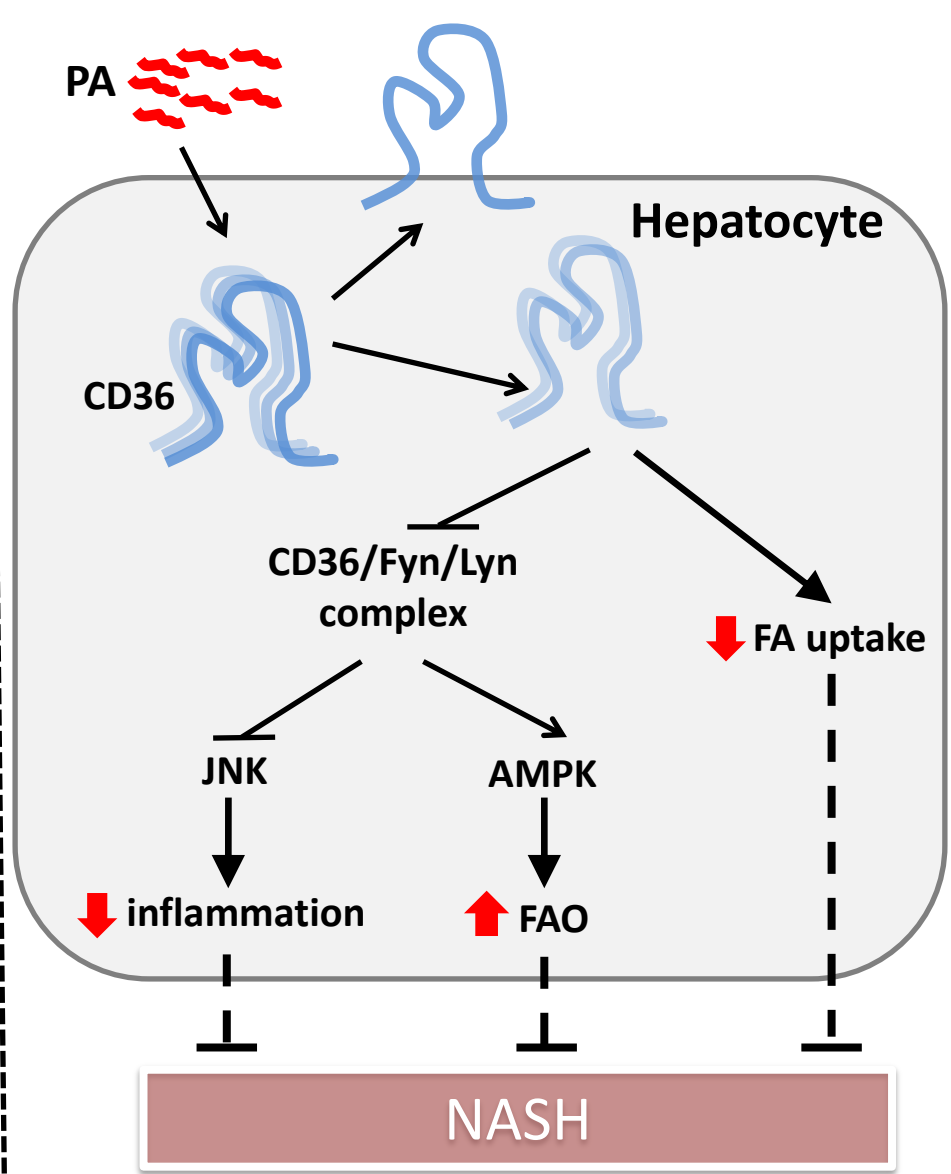


● cystein  
~ Palmitic acid

**+ CD36 palmitoylation**



**- CD36 palmitoylation**



**Highlights**

(Ms No. JHEPAT-D-16-02130R1)

- CD36 palmitoylation is increased in NASH.
- Palmitoylated CD36 facilitates FA uptake and lipid accumulation.
- Palmitoylated CD36 activates JNK/NF- $\kappa$ B by enhancing the formation of the CD36/Lyn/Fyn complex.
- Palmitoylated CD36 impairs FA  $\beta$ - oxidation.
- Inhibition of CD36 palmitoylation prevents NASH development.

ACCEPTED MANUSCRIPT